# Flow of Nonuniformly Stratified Fluid of Large Depth over Topography

by

Kevin S. Davis

B.M.E. Georgia Institute of Technology, 1997

Submitted to the Department of Mechanical Engineering in partial fulfillment of the requirements for the degree of

Master of Science in Mechanical Engineering

at the
Massachusetts Institute of Technology

June 1999



Signature of Author _____
Department of Mechanical Engineering
May 4, 1999

Certified by _____
Triantaphyllos R. Akylas
Thesis Supervisor

Accepted by _____
Ain A. Sonin
Chairman, Departmental Committee for Graduate Studies

# Flow of Nonuniformly Stratified Fluid of Large Depth over Topography

by

Kevin S. Davis

Submitted to the Department of Mechanical Engineering on May 4, 1999 in partial fulfillment of the requirements for the degree of Master of Science in Mechanical Engineering

## Abstract

This thesis extends Long's model (Long 1953) for steady flow of a hydrostatic, Boussinesq, uniformly stratified fluid of large depth over topography, to accommodate two layers of uniform stratification and subsequently variable stratification. The two-layer solution follows the work by Durran (1992) and is obtained in a piecewise fashion with the appropriate matching conditions at the stratification interface. The variable stratification solution is obtained by resolving the vertical dependence of the stratification with a numerical 'shooting' or integration technique. Consequently, this solution is in general not fully analytical. These techniques are applied to small and finite-amplitude two-dimensional problems as well as small-amplitude three-dimensional problems.

The two-layer solution, when implemented, encounters many of the same numerical problems seen by Durran. However, the variable stratification allows for the close approximation of the two-layer situation and does not suffer from the same convergence problems. Further, variable stratification allows for general stratification profiles. The effect known as tropopause tuning is diminished as the stratification interface continuously varies over a transition region. Similar results are also obtained for the small-amplitude three-dimensional case.

Thesis Supervisor: Triantaphyllos R. Akylas
Title: Professor of Mechanical Engineering

# Acknowledgements

The author would like to thank Professor T. R. Akylas for his guidance and advice in the development of this study.

This work was supported in part by the Air Force Office of Scientific Research Grant F49620-98-1-0388.

# Contents

# List of Figures

# Chapter 1

# General Introduction

Many forms of life on Earth, including our own, spend a large portion of their existence in the atmosphere or the ocean. Because of this dependence, the study of these vast fluid bodies is of practical interest. For example, the motion of the atmosphere can induce drastic changes in local weather conditions. This change can in turn have a dramatic effect on the local biosphere. Heavy precipitation, high-speed wind, or extreme temperatures can cause crop damage. More serious situations, such as a major flood or a tornado can even cause death. By studying the motion of the atmosphere, it may be possible to better predict changing weather patterns. Another example of the practical interest of the atmosphere or the oceans is the occurrence of turbulence. The study of turbulence is of particular concern to the structural development of aircraft, whether for commercial or military use. There are many other such practical interests that drive the study of the atmosphere and the oceans. Undoubtedly, this area will remain an active area of research for many years to come.

The atmosphere and the ocean, as well as many other fluid bodies, are stratified so that the density varies with height. Such a stratified fluid, in the presence of a gravity field, can support internal waves. In particular, this thesis focuses on internal waves excited by the presence of topography in a stratified fluid. In general, the density stratification can be uniform, discontinuous, or continuously varying with height. A convenient measure of the density stratification is the Brunt-Väisälä frequency, $N$. For an incompressible fluid with density, $\rho$, that varies in the vertical direction, $z$, the Brunt-Väisälä frequency is defined as

$$N^2(z) = -\frac{g}{\rho}\frac{d\rho}{dz}. \tag{1.1}$$

This quantity represents the frequency at which a small fluid element oscillates when slightly displaced from its equilibrium position. As indicated by Equation 1.1, an exponential density profile gives rise to a constant $N$. Typically, dimensional values for $N$ in the atmosphere are approximately $10^{-2}$ $sec^{-1}$. Note that for atmospheric flows, the density stratification is usually not entirely constant with elevation but may have two or more layers of more or less constant $N$. Typically, there are two atmospheric layers of interest. The lower layer, referred to as the troposphere, varies in height from approximately 8 km at the Earth's poles to approximately 18 km at the equator. The upper layer, referred to as the stratosphere, is separated from the troposphere by a boundary called the tropopause. A plot of typical Brunt-Väisälä frequency data is given in Section 2.4. The effects of a variable Brunt-Väisälä frequency and the tropopause profile on internal waves are centerpieces of this thesis.

This thesis also focuses on a fluid of large depth, such as the vastness of the atmosphere or the ocean. This situation prevents energy from being trapped in the fluid. Therefore, the energy supplied by the topography must propagate upward, away from the topography. This condition gives rise to a special boundary condition called a radiation condition, which is discussed in detail later in the thesis.

This thesis attempts to isolate the effects of gravity-induced waves, since they are the direct result of the stratification, and thus neglects the interaction of many other effects. For example, this thesis assumes centrifugal and Coriolis effects due to the earth's rotation are negligible. In geophysical flows, centrifugal effects are smaller by a factor of $10^{-3}$ or so. Coriolis effects are also small relative to gravity effects. This assumption can be quantified by

examining the dimensionless quantity called the Rossby number. The Rossby number, $Ro$, in terms of the angular speed, $\Omega$, the flow velocity, $U$, and the length scale, $L$, is defined as

$$Ro = \frac{U}{\Omega L}. \tag{1.2}$$

For typical values, the Rossby number is quite large, thus indicating that rotational effects can be neglected. Also, the effects of acoustical waves can be neglected. Acoustical waves have a typical frequency range of 1 to $10^4$ Hz, with a corresponding time scale of 1 to $10^{-4}$ seconds. Since gravity waves have time scales on the order of minutes and hours, acoustical wave interaction can be neglected.

Further assumptions regarding the background flow itself are also made. The large length scales present in this problem result in a large Reynolds number, indicating that viscous effects are restricted to a small layer close to the topography. Therefore, in the absence of flow separation, an inviscid model is sufficient to capture the physics of the internal waves. Further, the background flow is assumed to satisfy the Richardson number criterion for linear shear flow stability, $Ri > 1/4$ (Drazin & Reid 1981, p. 328). The Richardson number is a common measure for the effects of shear relative to the effects of stratification. For this situation, the Richardson number is defined as

$$Ri = \frac{N^2(z)}{\left(\frac{dU}{dz}\right)^2} = \frac{-\frac{g}{\rho}\frac{d\rho}{dz}}{\left(\frac{dU}{dz}\right)^2}. \tag{1.3}$$

As in most natural flows, the Prandtl number is large and thus diffusive effects are negligible. Also the Mach number is small and therefore the flow can be treated as incompressible. The flow is also assumed to have evolved from rest to a steady state without wave breaking. Finally,

the flow is also assumed to follow the Boussinesq and hydrostatic approximations. These approximations and their associated parameters are discussed in detail in Section 2.1.

Most analytical solutions in this area stem from Long (1953), who first studied this problem in detail and devised an analytical model. In Long's model, a constant upstream velocity profile and a constant Brunt-Väisälä frequency profile cause the two-dimensional form the governing equations to reduce to a single linear equation. Further, an analytical solution for this model is easily attainable even for finite-amplitude topography. However, Long's model predicts a critical topography amplitude at which the streamlines become vertical in regions of the flow field thereby invalidating the governing assumption of no breaking.

Many publications have since followed Long's work through analytical development, numerical verification, and experimental verification of the model. Some of the more noteworthy publications in the context of this thesis include Long (1955), Long (1959), Yih (1960), Drazin (1961), Drazin & Moore (1967), Yih (1967), Miles (1969), McIntyre (1972), Baines (1977), Lilly & Klemp (1979), Smith (1980), Peltier & Clark (1983), Baines (1987), and Smith (1989). In addition, the book, *Topographic effects in stratified flows*, by Baines (1995) is particularly useful.

Without question, Long's model is of paramount importance to the study of stratified flow. Nonetheless, a uniform stratification profile does not accurately approximate either the atmosphere or the ocean. Consequently, Long's model has been extended to two layers of uniform stratification. The two-layer model has been extensively studied by Durran (1992). While allowing for more general stratification profiles, this situation introduces a nonlinear boundary condition for the finite-amplitude case. This nonlinear boundary condition requires

iteration to obtain a solution. In addition, the two-layer profile allows for a phenomenon called tropopause tuning, which is another centerpiece for this thesis.

Further extension of Long's model to variable stratification profiles allows for an even more accurate approximation of real world stratification profiles. This extension is accomplished in this thesis by relaxing the requirement of a fully analytical solution but without resorting to direct numerical simulation. The varying Brunt-Väisälä frequency is resolved using a 'shooting' or integration technique to determine the solution. As will be shown, this situation has many benefits over the single or two-layer solutions.

For the analogous three-dimensional problem, there is currently no analytical solution for finite-amplitude topography. This problem does not reduce to a linear form as in Long's model. However, the small-amplitude case does have a formal solution (Baines 1995, p. 348). Therefore, this thesis also explores the parallel extension of the three-dimensional small-amplitude problem to include variable stratification profiles.

The remaining chapters of this thesis proceed as follows. Chapter 2 focuses on two-dimensional flow over small-amplitude and finite-amplitude topography. The governing equations are formulated and then solved for various stratification profiles. The resulting effects of the different profiles are also discussed. Chapter 3 focuses on three-dimensional flow over small topography. The governing equations are formulated and then solved for various stratification profiles. The resulting effects of the different profiles are discussed and compared to the two-dimensional results. The thesis concludes with some closing remarks in Chapter 4.

# Chapter 2

# Two-Dimensional Flow

This chapter focuses on two-dimensional flow of a stratified fluid of large depth over topography. This situation would be ideally represented in geophysical flows by very long topography spanwise to the flow direction, e.g. a long mountain range in the earth's atmosphere. The effect of topography of finite extent in the spanwise direction is discussed in Chapter 3.

This chapter begins by formulating Long's equation (Long 1953) for nonuniform stratification from the governing equations of motion. Next, the classic Boussinesq, hydrostatic, uniformly stratified solution, often referred to as Long's solution, is presented. This solution is presented for small-amplitude as well as finite-amplitude topography. Both of these solutions are expanded to the case of two layers of uniform stratification and to the more general case of a single layer of variable stratification. A discussion of these solutions concludes the chapter. Included in this discussion are comments on the comparison of the small-amplitude with the finite-amplitude solutions and on the effect of tropopause tuning in various stratification profiles.

## 2.1 Governing Equations

Consider the flow of a steady, incompressible, and inviscid fluid in the absence of rotational effects. The governing equations are

$$\nabla \cdot \mathbf{u} = 0 \tag{2.1}$$

$$\mathbf{u} \cdot \nabla \rho = 0 \tag{2.2}$$

$$\rho \mathbf{u} \cdot \nabla \mathbf{u} = -\nabla p + \rho \mathbf{g} \tag{2.3}$$

where $\rho$ is the local fluid density, **u** is the local velocity vector, $p$ is the local pressure, and **g** is the downward pointing gravitational acceleration. Equations 2.1 – 2.3 respectively represent incompressibility, mass balance, and momentum balance. In this chapter, the coordinate system is limited to two dimensions, $x$ and $z$. The $x$-direction is horizontal and the $z$-direction is vertical. Using this coordinate system, Equations 2.1 – 2.3 reduce to

$$u_x + w_z = 0 \tag{2.4}$$

$$u\rho_x + w\rho_z = 0 \tag{2.5}$$

$$\rho(uu_x + wu_z) = -p_x \tag{2.6}$$

$$\rho(uw_x + ww_z) = -p_z - \rho g \tag{2.7}$$

These equations can be non-dimensionalized by the following substitution,

$$x = L\tilde{x}\,,\quad z = \frac{U_0}{N_0}\tilde{z}\,,\quad u = U_0\tilde{u}\,,\quad w = \frac{U_0^2}{LN_0}\tilde{w}\,,\quad \rho = \rho_0\tilde{\rho}\,,\quad p = \frac{gU_0\rho_0}{N_0}\tilde{p}\,. \tag{2.8}$$

Here, $L$ represents a characteristic length scale such as the topography half-width, $N_0$ represents a characteristic Brunt-Väisälä frequency, $U_0$ represents the uniform free-stream velocity, and $\rho_0$ represents the characteristic free-stream density. After dropping the tildes, the dimensionless equations are

$$u_x + w_z = 0\,, \tag{2.9}$$

$$u\rho_x + w\rho_z = 0\,, \tag{2.10}$$

$$\beta\rho(uu_x + wu_z) = -p_x\,, \tag{2.11}$$

$$\beta\rho(uw_x + ww_z) = -\mu^{-2}(p_z + \rho). \tag{2.12}$$

As indicated in these equations, two dimensionless parameters arise, $\beta$ and $\mu$. These parameters are defined as

$$\beta = \frac{N_0 U_o}{g},\ \mu = \frac{U_0}{N_0 L}. \tag{2.13}$$

The first parameter is called the Boussinesq parameter and controls stratification effects. The second parameter is called the longwave parameter and controls dispersive effects. Further assumptions for both of these parameters will be made below. A streamfunction can be introduced as follows

$$u = \Psi_z,\ w = -\Psi_x. \tag{2.14}$$

By introducing this stream function, the incompressibility equation is automatically satisfied, and only the mass and momentum balance equations remain,

$$\Psi_z \rho_x - \Psi_x \rho_z = 0, \tag{2.15}$$

$$\beta\rho\left(\Psi_z \Psi_{zx} - \Psi_x \Psi_{zz}\right) = -p_x, \tag{2.16}$$

$$\beta\rho\left(-\Psi_z \Psi_{xx} + \Psi_x \Psi_{xz}\right) = -\mu^{-2}\left(p_z + \rho\right). \tag{2.17}$$

Equation 2.15 can be written in Jacobian form as

$$J\{\rho, \Psi\} = 0. \tag{2.18}$$

The Jacobian, $J\{\}$, for two arbitrary functions, $A$(x,z) and $B$(x,z), in this situation is defined as

$$J\{A, B\} = A_x B_z - A_z B_x. \tag{2.19}$$

As expected, Equation 2.18 indicates that the density is a function of $\Psi$ alone, and thus a constant along a streamline. The pressure can be eliminated from Equations 2.16 and 2.17 by cross-differentiation to yield a single momentum equation,

$$\rho_z\left(\Psi_z \Psi_{zx} - \Psi_x \Psi_{zz}\right) + \rho\left(\Psi_z \Psi_{zx} - \Psi_x \Psi_{zz}\right)_z$$

$$+ \mu^2 \rho_x\left(\Psi_z \Psi_{xx} - \Psi_x \Psi_{xz}\right) + \mu^2 \rho\left(\Psi_z \Psi_{xx} - \Psi_x \Psi_{xz}\right)_x - \frac{\rho_x}{\beta} = 0. \tag{2.20}$$

Collecting terms and substituting from Equation 2.15 gives

$$\rho\left[\left(\Psi_{zz}+\mu^2\Psi_{xx}\right)\Psi_z-\left(\Psi_{zz}+\mu^2\Psi_{xx}\right)\Psi_x\right]$$

$$+\rho_z\left(\Psi_z\Psi_{zx}+\mu^2\Psi_x\Psi_{xx}\right)-\rho_x\left(\Psi_z\Psi_{zz}+\mu^2\Psi_x\Psi_{xz}+\beta^{-1}\right)=0. \tag{2.21}$$

Converting this equation to Jacobian form as before gives,

$$\rho J\left\{\Psi_{zz}+\mu^2\Psi_{xx},\Psi\right\}+J\left\{\frac{1}{2}\left(\Psi_z^2+\mu^2\Psi_x^2\right)+\frac{z}{\beta},\rho\right\}=0. \tag{2.22}$$

Since, from Equation 2.18, $\rho$ is a function of $\Psi$, the second Jacobian in the above equation can be manipulated to give

$$\rho J\left\{\Psi_{zz}+\mu^2\Psi_{xx},\Psi\right\}+\frac{\rho_\Psi}{\beta\rho}J\left\{z+\frac{\beta}{2}\left(\Psi_z^2+\mu^2\Psi_x^2\right),\Psi\right\}=0. \tag{2.23}$$

The coefficient of the second term in the above equation is the dimensionless Brunt-Väisälä frequency, *N*, which for this situation is defined as

$$N^2(\Psi)=\frac{\rho_\Psi}{\beta\rho}. \tag{2.24}$$

Thus Equation 2.23 gives a single Jacobian equation for $\Psi$,

$$J\left\{\Psi_{zz}+\mu^2\Psi_{xx}-N^2(\Psi)\left[z+\frac{\beta}{2}\left(\Psi_z^2+\mu^2\Psi_x^2\right)\right],\Psi\right\}=0. \tag{2.25}$$

Equation 2.25 implies

$$\Psi_{zz}+\mu^2\Psi_{xx}-N^2(\Psi)\left[z+\frac{\beta}{2}\left(\Psi_z^2+\mu^2\Psi_x^2\right)\right]=G(\Psi). \tag{2.26}$$

The function $G(\Psi)$ is determined by examining the flow far upstream from the disturbance. Far upstream the flow is assumed to be undisturbed and $\Psi=z$. McIntyre (1972) and Baines (1977) discuss the assumption of no upstream influence in more detail. Therefore, Equation 2.26 reduces to

$$G(\Psi)=-N^2(\Psi)\left(\Psi+\frac{\beta}{2}\right). \tag{2.27}$$

Substituting Equation 2.27 in Equation 2.26 for $G(\Psi)$ gives

$$\Psi_{zz}+\mu^2\Psi_{xx}-N^2(\Psi)\left[z-\Psi+\frac{\beta}{2}\left(\Psi_z^2+\mu^2\Psi_x^2-1\right)\right]=0. \tag{2.28}$$

Equation 2.28 is often referred to as Long's equation for general stratification. For a Bousinesq fluid, i.e. $\beta\to 0$, the equation reduces to

$$\Psi_{zz}+\mu^2\Psi_{xx}+N^2(\Psi)(\Psi-z)=0. \tag{2.29}$$

In the hydrostatic limit, $\mu\to 0$, the equation further reduces to

$$\Psi_{zz}+N^2(\Psi)(\Psi-z)=0. \tag{2.30}$$

Substituting $\Psi=\psi+z$ and thereby working with the streamline perturbation yields the convenient form

$$\psi_{zz}+N^2(\psi+z)\psi=0. \tag{2.31}$$

Solutions to this equation depend upon the profile of the stratification as indicated by the appearance of $N(\psi+z)$.

In addition, there are two boundary conditions. First, there is no normal flow on the surface of the topography. For finite topography in the original dimensional variables, the boundary condition is

$$\mathbf{u}\cdot\hat{\mathbf{n}}=0. \tag{2.32}$$

Introducing $f(x)$ as the shape of the topography with a characteristic height, $h$, gives

$$w(x,f)-u(x,f)f_x=0. \tag{2.33}$$

Since the flow is assumed to be undisturbed upstream and downstream of the topography, the topography must be locally confined. In this chapter, the topography used is given by

$$f(x)=\frac{h}{\left(1+x^2\right)^{3/2}}. \tag{2.34}$$

The 3/2 exponent in the denominator is retained here for comparison to the three-dimensional topography used in Chapter 3. Scaling Equation 2.33 as before and scaling $f$(x) by $h$ gives

$$w(x,\varepsilon f)-u(x,\varepsilon f)\varepsilon f_x=0. \tag{2.35}$$

The resulting dimensionless parameter, $\varepsilon$, is defined as

$$\varepsilon=\frac{hN_0}{U_0}. \tag{2.36}$$

This parameter effectively controls the amplitude of the response. Introducing the streamfunction as before gives

$$-\Psi_x(x,\varepsilon f)-\Psi_z(x,\varepsilon f)\varepsilon f_x=0. \tag{2.37}$$

Equation 2.37 represents the total derivative of $\Psi$ evaluated at $z=\varepsilon f$. Thus, the boundary condition becomes

$$\Psi(x,\varepsilon f)=const. \tag{2.38}$$

As expected, this result indicates that the topography is a line of constant $\Psi$ or a streamline. Since the choice of the constant is arbitrary, zero is chosen without a loss of generality. Introducing the streamline perturbation, $\psi$, then gives

$$\psi(x,\varepsilon f)=-\varepsilon f. \tag{2.39}$$

In the case of small-amplitude topography, i.e. when $\varepsilon\to 0$, this boundary condition reduces to

$$\psi(x,0)=-\varepsilon f. \tag{2.40}$$

The small-amplitude result is analogous to applying the boundary condition at the undisturbed height $z=0$ instead of on the topography. Application of the small-amplitude boundary condition will be presented for each stratification profile.

The second boundary condition is satisfied as $z \to \infty$. Since the flow is steady, energy from the topography must be radiated outwards. This type of boundary condition is often referred to as the radiation condition. This condition is met by insuring that the vertical group velocity is positive. Defining $k$ as the horizontal wavenumber and $m$ as the vertical wavenumber, the dispersion relation for hydrostatic flow is (Baines 1995, p. 181)

$$\omega(k) = k - \frac{\mathrm{sgn}(m)Nk}{m}. \tag{2.41}$$

The vertical group velocity is then given by

$$c_g\Big|_z = \frac{\partial \omega}{\partial m} = \frac{\mathrm{sgn}(m)Nk}{m^2}. \tag{2.42}$$

For the vertical group velocity to be positive,

$$km > 0. \tag{2.43}$$

Application of the radiation condition is further developed specifically for the uniform stratification case in Section 2.2.

As mentioned above, the solution depends upon the profile of the stratification. In Section 2.2, a single uniformly stratified layer is examined. This solution is extended in Section 2.3 for two layers of uniform stratification and extended further in Section 2.4 to variable stratification.

## 2.2 Single Layer of Uniform Stratification

The simplest stratification profile is a single semi-infinite layer of uniform stratification, i.e. $N(\psi + z) = N$. This problem is the classical Long's solution. For this situation, Equation 2.31 is linear even for the finite-amplitude case. Solutions to Equation 2.31 take the form

$$\psi(x,z) = p(x)\sin(Nz) + q(x)\cos(Nz). \tag{2.44}$$

The functions $p(x)$ and $q(x)$ are found by applying the lower boundary condition and the radiation condition as mentioned in Section 2.1.

To impose the radiation condition, consider the solution in Equation 2.44 in Fourier integral form,

$$\psi(x,z)=\frac{1}{2}\int_{-\infty}^{\infty}[\hat{q}(k)-i\hat{p}(k)]e^{i(kx+mz)}dk+\frac{1}{2}\int_{-\infty}^{\infty}[\hat{q}(k)+i\hat{p}(k)]e^{i(kx-mz)}dk\,. \tag{2.45}$$

To satisfy the radiation condition as stated in Equation 2.43, the first integral must vanish for $k<0$ and the second integral must vanish for $k>0$. Satisfying these criteria yields

$$\hat{q}(k)=i\hat{p}(k) \text{ for } k<0, \tag{2.46}$$

$$\hat{q}(k)=-i\hat{p}(k) \text{ for } k>0. \tag{2.47}$$

These constraints can be written more compactly as

$$\hat{q}(k)=-i\,\mathrm{sgn}(k)\hat{p}(k). \tag{2.48}$$

Converting to the real domain gives

$$p(x)=H[q(x)], \tag{2.49}$$

where $H[]$ is the Hilbert transform.

Next, consider imposing the small-amplitude version of the lower boundary condition. Equation 2.40 becomes simply

$$\psi(x,0)=q(x)=-\varepsilon f(x). \tag{2.50}$$

Thus the solution for the small-amplitude case is known. Alternatively, impose the finite-amplitude version of the lower boundary condition. For this case, Equation 2.39 becomes

$$\psi(x,\varepsilon f)=p(x)\sin(N\varepsilon f)+q(x)\cos(N\varepsilon f)=-\varepsilon f\,. \tag{2.51}$$

Substituting from Equation 2.49 for $p(x)$ yields a single integral equation for $q(x)$,

$$q(x)\cos(N\varepsilon f)+H[q(x)]\sin(N\varepsilon f)=-\varepsilon f\,. \tag{2.52}$$

This analysis agrees with Lilly & Klemp (1979) and others. By solving Equation 2.52 for $q(x)$, the finite-amplitude solution is known. As $\varepsilon \to 0$, Equation 2.52 reduces simply to

$$q(x) = -\varepsilon f , \tag{2.53}$$

thus recovering the small-amplitude result from Equation 2.50.

Equation 2.52 and Equation 2.53 can be easily solved. The small-amplitude solution is straightforward from Equation 2.53. The finite-amplitude solution is easily found by discretizing Equation 2.52 into a linear system.

## 2.3 Two Layers of Uniform Stratification

Now consider a layer of finite height with uniform stratification, $N(\psi + z) = N_L$, above which is a semi-infinite layer with uniform stratification, $N(\psi + z) = N_U$. This profile can more closely approximate the tropopause in the earth's atmosphere than the single layer solution presented in Section 2.2.

The governing equations presented in Section 2.1 are valid in each layer. Further, the solution in each layer will take the form presented in Section 2.2. However, the solutions for the small-amplitude and finite-amplitude cases differ significantly. The difference is partly due to the lower boundary condition as in the single layer solutions, but is largely due to the interface between the two layers. Specifically, the finite-amplitude solution is nonlinear because the exact location of the interface depends upon the solution. Consequently, the method for each case varies and will therefore be presented separately.

### 2.3.1 Small-Amplitude

For the small-amplitude case, the stratification depends on $z$ only. Therefore the interface

is at a constant height, $z^*$. The solution can then be constructed from a solution in the lower layer, $\psi_L$, and a solution in the upper layer, $\psi_U$,

$$\psi_L(x,z) = p(x)\sin(N_L z) + q(x)\cos(N_L z) \quad \text{for} \quad 0 < z < z^*, \tag{2.54}$$

$$\psi_U(x,z) = r(x)\sin[N_U(z-z^*)] + s(x)\cos[N_U(z-z^*)] \quad \text{for} \quad z > z^*. \tag{2.55}$$

To determine $p(x)$, $q(x)$, $r(x)$, and $s(x)$, a total of four boundary conditions are needed. First, the radiation condition must be satisfied as $z \to \infty$. In the upper layer, the radiation condition is simply

$$r(x) = H[s(x)]. \tag{2.56}$$

Next, continuity requires two matching conditions at the interface. At $z = z^*$, the velocity and its derivative are continuous. These conditions can be expressed in terms of the streamfunctions,

$$\psi_L(x,z^*) = \psi_U(x,z^*), \tag{2.57}$$

$$\frac{\partial \psi_L}{\partial z}(x,z^*) = \frac{\partial \psi_U}{\partial z}(x,z^*). \tag{2.58}$$

After the appropriate differentiation and substitution, these matching conditions become

$$s(x) = p(x)\sin(N_L z^*) + q(x)\cos(N_L z^*), \tag{2.59}$$

$$r(x) = \frac{N_L}{N_U}[p(x)\cos(N_L z^*) - q(x)\sin(N_L z^*)]. \tag{2.60}$$

Finally, the lower boundary condition in small-amplitude form is

$$\psi_L(x,0) = q(x) = -\varepsilon f\,. \tag{2.61}$$

Thus there are four equations, Equations 2.56, 2.59, 2.60, and 2.61, to solve for the four unknowns, $p(x)$, $q(x)$, $r(x)$, and $s(x)$. Combining these four equations yields a single integral equation for $p(x)$,

$$N_L \cos(N_L z^*)p(x) - N_U \sin(N_L z^*)H[p(x)]$$

$$= -N_L \sin(N_L z^*)\varepsilon f - N_U \cos(N_L z^*)H[\varepsilon f]. \tag{2.62}$$

Solving Equation 2.62 can be done by discretizing the equation into a linear system.

### 2.3.2 Finite-Amplitude

For the finite-amplitude case, the stratification depends upon $\psi + z$. Therefore the interface is at a constant value of $\Psi^*$, i.e. on a particular streamline, such that

$$\Psi^* = z^*(x) + \psi(x, z^*(x)). \tag{2.63}$$

Since the location of this interfacial streamline is not known apriori, the problem is nonlinear. However, the equations within each layer are linear and the solution takes a form similar to the small-amplitude case,

$$\psi_L(x,z) = p(x)\sin(N_L z) + q(x)\cos(N_L z) \text{ for } 0 < \psi(x,z) + z < \Psi^*, \tag{2.64}$$

$$\psi_U(x,z) = r(x)\sin[N_U(z - z^*)] + s(x)\cos[N_U(z - z^*)] \text{ for } \psi(x,z) + z > \Psi^*. \tag{2.65}$$

Nonetheless, an iterative scheme is required to determine $p(x)$, $q(x)$, $r(x)$, and $s(x)$. First, an initial guess for $\psi(x,z^*)$ is required. One suitable initial guess is $\psi(x,z^*)$ from the equivalent small-amplitude problem. Next, the radiation condition is applied in the upper layer. Taking the derivative of Equation 2.65 gives

$$\frac{\partial \psi_U}{\partial z}(x,z) = N_U \{r(x)\cos[N_U(z - z^*)] - s(x)\sin[N_U(z - z^*)]\}. \tag{2.66}$$

Solving Equation 2.65 and Equation 2.66 for $r(x)$ and $s(x)$ gives

$$r(x) = \psi_U \sin[N_U(z - z^*)] + \frac{1}{N_U}\frac{\partial \psi_U}{\partial z}\cos[N_U(z - z^*)], \tag{2.67}$$

$$s(x) = \psi_U \cos[N_U(z - z^*)] - \frac{1}{N_U}\frac{\partial \psi_U}{\partial z}\sin[N_U(z - z^*)]. \tag{2.68}$$

Imposing the radiation condition in the upper layer and collecting terms gives

$$\cos[N_U(z-z^*)]\frac{\partial \psi_U}{\partial z} + H\left[\sin[N_U(z-z^*)]\frac{\partial \psi_U}{\partial z}\right]$$

$$= -N_U \sin[N_U(z-z^*)]\psi_U + N_U H[\cos[N_U(z-z^*)]\psi_U]. \tag{2.69}$$

Next, impose the matching conditions at $z = z^*(x)$. Evaluating Equation 2.69 at $z^*(x)$ gives simply

$$\frac{\partial \psi_U}{\partial x}(x, z^*) = N_U H[\psi_U(x, z^*)]. \tag{2.70}$$

Differentiating Equation 2.64 with respect to $z$ gives

$$\frac{\partial \psi_L}{\partial z}(x, z) = N_L[p(x)\cos(N_L z) - q(x)\sin(N_L z)]. \tag{2.71}$$

Solving Equation 2.64 and Equation 2.71 for $p(x)$ and $q(x)$ gives

$$p(x) = \psi_L \sin(N_L z) + \frac{1}{N_L}\frac{\partial \psi_L}{\partial z}\cos(N_L z), \tag{2.72}$$

$$q(x) = \psi_L \cos(N_L z) - \frac{1}{N_L}\frac{\partial \psi_L}{\partial z}\sin(N_L z). \tag{2.73}$$

The constants, $p(x)$ and $q(x)$, can be found by evaluating Equations 2.72 and 2.73 at $z = z^*(x)$. Finally, check to insure the lower boundary condition is satisfied by evaluating

$$p(x)\sin(N\varepsilon f) + q(x)\cos(N\varepsilon f) + \varepsilon f = 0. \tag{2.74}$$

In general, the lower boundary condition will not be satisfied and the initial guess will be updated accordingly. Thus, the iteration proceeds until convergence. For the solutions discussed in Section 2.5, Newton-Raphson iteration is employed.

The finite-amplitude solution obtained above agrees with the one presented by Durran (1992). Unfortunately, the behavior of the numerical procedure also agrees with Durran's results. Specifically, Durran's algorithm fails when the interface is an odd quarter lower wavelength above the topography. The above procedure also fails to converge for any of these

situations. Durran attributes this lack of convergence to a defect in the numerical algorithm. Since the variable stratification solution presented in Section 2.4.2 does converge when approximating this situation, Durran's reasoning seems correct. More precisely, the lack of convergence is most likely a defect in the method of the solution. Durran also mentions that his algorithm does not converge for cases when the interface is not near an odd quarter lower wavelength. This behavior is also apparent in the procedure described above. The procedure fails to converge for situations that are significantly nonlinear. The maximum value of $\varepsilon$ for the procedure to fail to converge varies, however it can be as low as 0.5~0.6. As Durran suggests, this result could indicate the development of a nonlinear resonance. However, since the variable stratification solution in Section 2.4.2 converges for the same situation, the lack of convergence is again most likely due to a defect in the method of the solution.

## 2.4 Variable Stratification

Now consider stratification that varies with height, i.e. $N = N(\psi + z)$. This situation accommodates general stratification profiles, which better approximates actual atmospheric conditions. For example, typical Brunt-Väisälä frequency data for the atmosphere above Korea, as observed by the Air Force Office of Scientific Research, is shown in Figure 2.1. Clearly, the data indicates that the atmosphere does not have a uniform stratification structure. As a first observation, the frequency is roughly centered about 0.01 Hz up to a height of 10 km. At this point there is a transition region up to a height of 15 km, above which the frequency is roughly centered about 0.02 Hz. To approximate this type of profile, a hyperbolic tangent is used,

$$N(\psi + z) = a + b\tanh[c(\psi + z - d)]. \tag{2.75}$$

The parameters, *a*, *b*, *c*, and *d*, are used simply to adjust the size, shape, and location of the profile. Other functions can be used, but this function allows for the approximation of the two-layer solution. In general the solution can not be written in a closed analytical form and therefore requires numerical computation. This complication in turn causes the small-amplitude and finite-amplitude boundary conditions to be more conveniently imposed using different techniques.

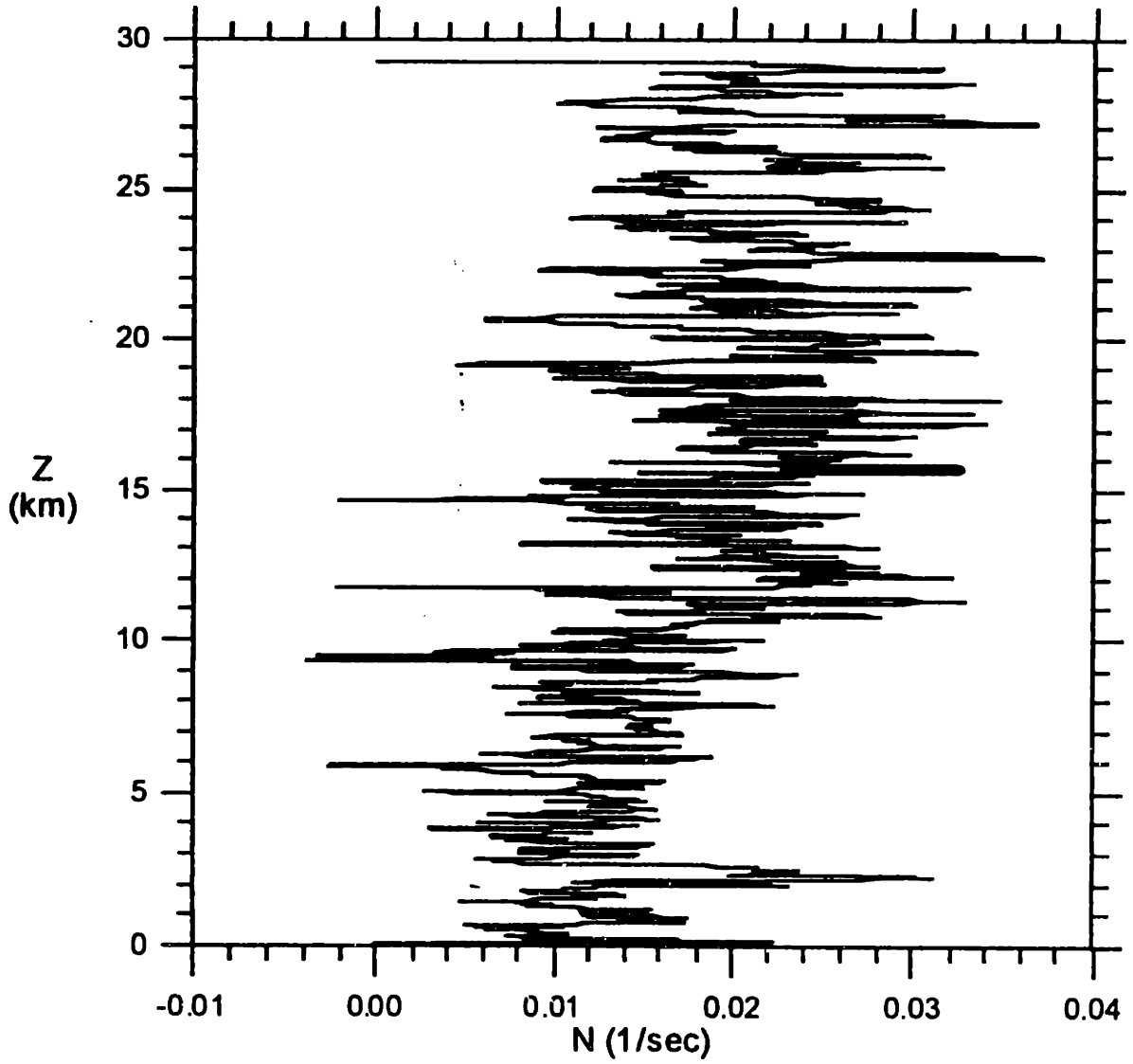


Figure 2.1: Typical atmospheric Brunt-Väisälä frequency data

### 2.4.1 Small-Amplitude

When considering the small-amplitude case, the solution can be posed using separation of variables. Introducing $\eta_1(z)$ and $\eta_2(z)$ yields a solution of the form

$$\psi(x,z) = p(x)\eta_1(z) + q(x)\eta_2(z). \tag{2.76}$$

Therefore, $\eta_1(z)$ and $\eta_2(z)$ are independent solutions of

$$\frac{d\eta(z)}{dz} + N^2(z)\eta(z) = 0. \tag{2.77}$$

Choosing the following 'initial' conditions for $\eta_1(z)$ and $\eta_2(z)$ automatically satisfies the lower boundary condition,

$$\eta_1(0) = 0, \quad \eta_2(0) = 1, \quad \frac{d\eta_1}{dz}(0) = 1, \quad \frac{d\eta_2}{dz}(0) = 0. \tag{2.78}$$

This formulation effectively determines $q(x)$. Next, $\eta_1(z)$ and $\eta_2(z)$ can be found by 'shooting' to the top of the numerical domain. For the solutions presented in Section 2.5, a fourth-order Runge-Kutta scheme is used. Applying the radiation condition will yield the remaining unknown, $p(x)$. However, the radiation condition was derived specifically for uniform stratification. That form of the radiation condition, as derived in Section 2.1 and applied in Sections 2.2 and 2.3, can be used here by requiring $N(z)$ to asymptote to a constant, $N_\infty$, as $z \to \infty$. To implement the radiation condition in this manner, a fictitious upper layer with uniform stratification, $N = N_\infty$, can be introduced at the top of the computational domain, $z = z_\infty$. Note that $z_\infty$ must be sufficiently high. In this layer, the solution takes the usual form,

$$\psi_\infty(x,z) = r(x)\sin[N_\infty(z - z_\infty)] + s(x)\cos[N_\infty(z - z_\infty)]. \tag{2.79}$$

As discussed in Section 2.3, there are also two matching conditions,

$$\psi(x,z_\infty) = \psi_\infty(x,z_\infty), \tag{2.80}$$

$$\frac{\partial \psi}{\partial z}(x, z_\infty) = \frac{\partial \psi_\infty}{\partial z}(x, z_\infty). \tag{2.81}$$

These matching conditions in turn yield,

$$s(x) = p(x)\eta_1(z_\infty) + q(x)\eta_2(z_\infty), \tag{2.82}$$

$$r(x) = \frac{1}{N_\infty}\left[ p(x)\frac{d\eta_1}{dz}(z_\infty) + q(x)\frac{d\eta_2}{dz}(z_\infty)\right]. \tag{2.83}$$

Most importantly, the radiation condition in the upper layer is

$$r(x) = H[s(x)]. \tag{2.84}$$

Manipulating Equations 2.40, 2.82, 2.83, and 2.84 gives a single integral equation for $p(x)$,

$$\frac{d\eta_1}{dz}(z_\infty)p(x) - N_\infty \eta_1(z_\infty)H[p(x)] = \frac{d\eta_2}{dz}(z_\infty)\varepsilon f - N_\infty \eta_2(z_\infty)H[\varepsilon f]. \tag{2.85}$$

This equation is easily solvable by discretizing into a linear system.

### 2.4.2 Finite-Amplitude

When considering the finite-amplitude case, the solution is nonlinear and thus requires an iterative scheme. First, the radiation condition is implemented by introducing a fictitious upper layer as before,

$$\psi_\infty(x, z) = r(x)\sin[N_\infty(z - z_\infty)] + s(x)\cos[N_\infty(z - z_\infty)]. \tag{2.86}$$

Even though the situation under consideration here is the finite-amplitude case, introducing the upper layer at a constant height instead of on a specific streamline is acceptable. This reasoning is valid because $N$ has asymptotically reached a constant value and there is no appreciable variation present. The derivative with respect to $z$ in the upper layer is

$$\frac{\partial \psi_\infty}{\partial z} = N_\infty\{r(x)\cos[N_\infty(z - z_\infty)] - s(x)\sin[N_\infty(z - z_\infty)]\}. \tag{2.87}$$

Solving Equations 2.86 and 2.87 for $r(x)$ and $s(x)$ gives

$$r(x)=\psi\sin[N_\infty(z-z_\infty)]+\frac{1}{N_\infty}\frac{\partial\psi}{\partial z}\cos[N_\infty(z-z_\infty)], \tag{2.88}$$

$$s(x)=\psi\cos[N_\infty(z-z_\infty)]-\frac{1}{N_\infty}\frac{\partial\psi}{\partial z}\sin[N_\infty(z-z_\infty)]. \tag{2.89}$$

Imposing the radiation condition from Equation 2.84 and evaluating the result at $z_\infty$ gives

$$\frac{\partial\psi}{\partial z}(x,z_\infty)=N_\infty H[\psi(x,z_\infty)]. \tag{2.90}$$

Thus for an initial guess for $\psi$ at the top of the numerical domain, the derivative there is given by Equation 2.90. These values can then be used to 'shoot' downward to the topography, parametrically in $x$. For the solutions presented in Section 2.5, a fourth-order Runge-Kutta scheme is used. On the topography, the solution is checked to agree with the lower boundary condition by evaluating

$$p(x)\sin(N\varepsilon f)+q(x)\cos(N\varepsilon f)+\varepsilon f=0. \tag{2.91}$$

In general, the boundary condition will not be satisfied and the initial guess can be updated using a Newton-Raphson scheme. The procedure is then iterated upon until convergence. In this fashion, the iteration scheme is very similar to the scheme employed for the two-layer finite-amplitude solution.

The main difference in the implementation of the variable stratification scheme and the two-layer scheme is that the variable stratification requires shooting. This additional step is numerically inexpensive but provides significant benefit. As mentioned before, the variable stratification allows for a wide variety of stratification profiles. In addition, the variable stratification numerical scheme does not suffer from the convergence problems that the two-layer scheme has, even when the profile is adjusted to closely resemble a two-layer discontinuity.

However, the height of the numerical domain for the variable stratification solution must be selected with care. An incorrect height can not only invalidate the reasoning governing the introduction of the fictitious upper layer, but can also cause the procedure to fail to converge. Since this height is not of physical significance, this limitation can be easily overcome by adjusting the height to a value in which the reasoning is valid and the procedure does converge.

## 2.5 Discussion

For the purposes of this discussion, the topography used is of the form in Equation 2.34. In addition, the variable stratification profile used is of the form in Equation 2.75. All of the figures shown in this section are in dimensionless form.

This section begins with a simple comparison of the small-amplitude and finite-amplitude solutions for each of the three stratification profiles. Next, the discussion focuses on the effects of tropopause tuning. Specifically, the effect of the placement of the tropopause will be examined. In addition, the variable stratification case allows for a discussion on the effect of the tropopause shape, i.e. a smooth transition instead of a sharp discontinuity.

### 2.5.1 Small-Amplitude vs. Finite-Amplitude

In Figure 2.2 a few streamlines are shown for a single layer of uniform stratification. In this plot, both the small-amplitude and finite-amplitude solutions are shown in dimensionless form for $N = 1$ and $\varepsilon = 0.75$. The lower dotted line indicates the topography. Note that the streamline pattern repeats in the vertical direction every $2\pi$, indicating the single vertical wavenumber, $m = 1$. There is a discrepancy between the small-amplitude and finite-amplitude solutions, which will vanish for smaller values of $\varepsilon$. The streamlines will become vertical for the

finite-amplitude case when $\varepsilon = 0.85$. At this point the solution indicates breaking, which violates the hydrostatic assumption. Solutions beyond $\varepsilon = 0.85$ are possible but they are physically meaningless. These results agree with Lilly & Klemp (1979) and others.

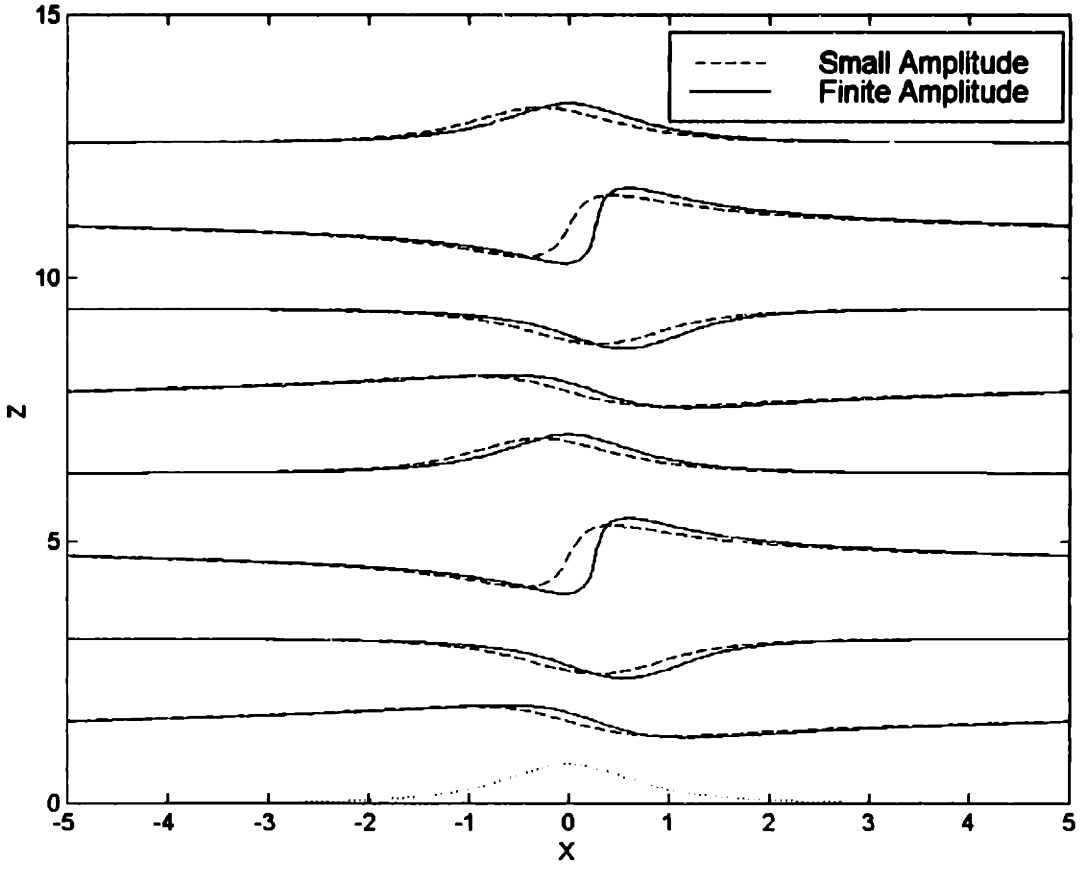


Figure 2.2: Streamlines for a single layer of uniform stratification.

In Figure 2.3 a few streamlines for two layers of uniform stratification are shown. In this figure, $N_L = 4/3$, $N_U = 2/3$, and $\varepsilon = 0.45$. This situation is unlike the earth's atmosphere in which $N$ typically increases with height. A more physically meaningful situation is presented in Section 2.5.2. The value for $\varepsilon$ is based on the average of $N_L$ and $N_U$. In this manner, the value is easily comparable to the variable stratification case. The lower dotted line is again the

topography. The upper dotted line represents the interfacial streamline between the two layers of stratification for the finite-amplitude case. This interface is at $\Psi^* = 2.83$ or 0.6 times the lower wavelength. For the small-amplitude case the interface is not shown but is at a constant height, $z^* = 2.83$ or 0.6 times the lower wavelength. As expected, the streamline pattern now repeats every $2\pi/N_L$ in the lower layer and every $2\pi/N_U$ in the upper layer. For the flow situations depicted, the small-amplitude and finite-amplitude solutions differ significantly. The nonlinearity appears to have a pronounced effect on the flow.

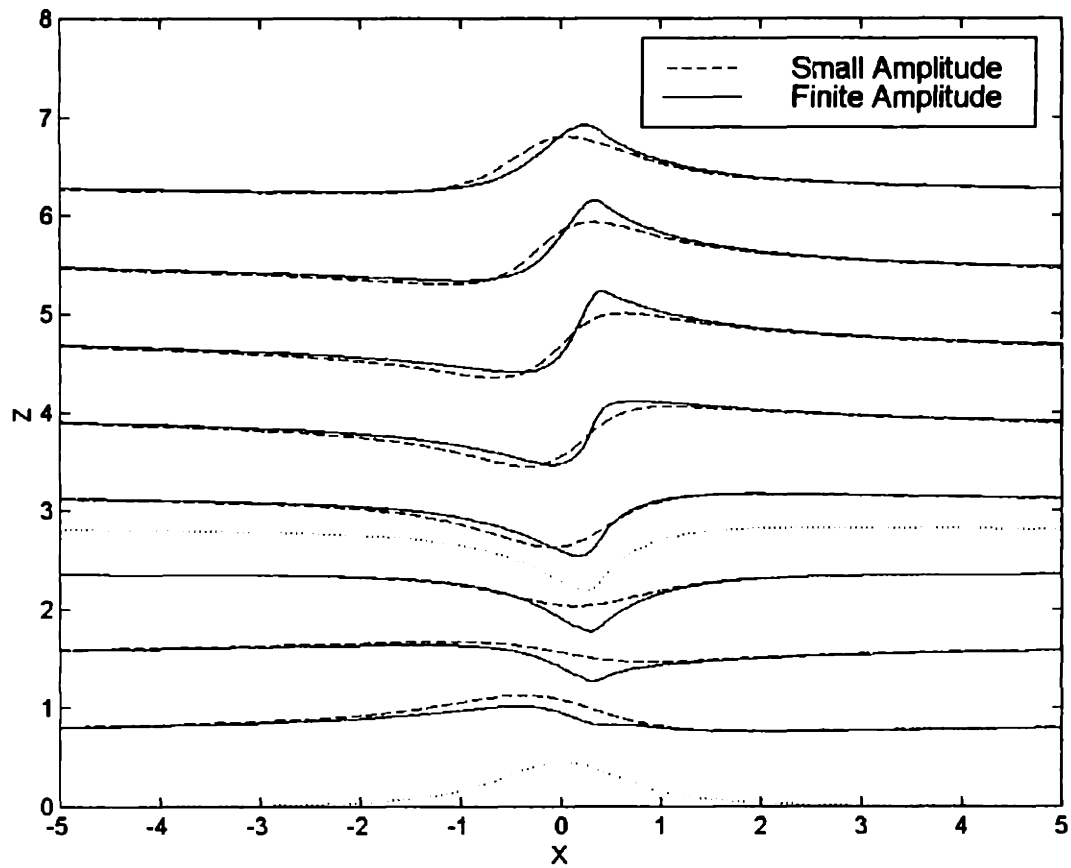


Figure 2.3: Streamlines for two layers of uniform stratification.

In Figure 2.4 a few streamlines for a layer of variable stratification are shown. The stratification profile used is of the form in Equation 2.75, with $a = 1$, $b = -1/3$, $c = 2$, and

$d = 2.83$. This situation is a continuously varying version of the two-layer solution presented above. As $c$ becomes large, the profile sharpens and the situation approximates the two-layer profile. In Figure 2.3, the amplitude is moderate with $\varepsilon = 0.45$, where $\varepsilon$ is based on the value of $a$. The lower dotted line again represents the topography. An interfacial streamline is of little physical importance for this situation. As expected, the streamline pattern repeats every $2\pi/N_L$ near the bottom of the layer, every $2\pi/N_U$ near the top of the layer, and varies with the stratification in the middle of the layer. Nonlinearity again appears to have a significant effect, however this effect has been diminished because of the continuously varying profile.

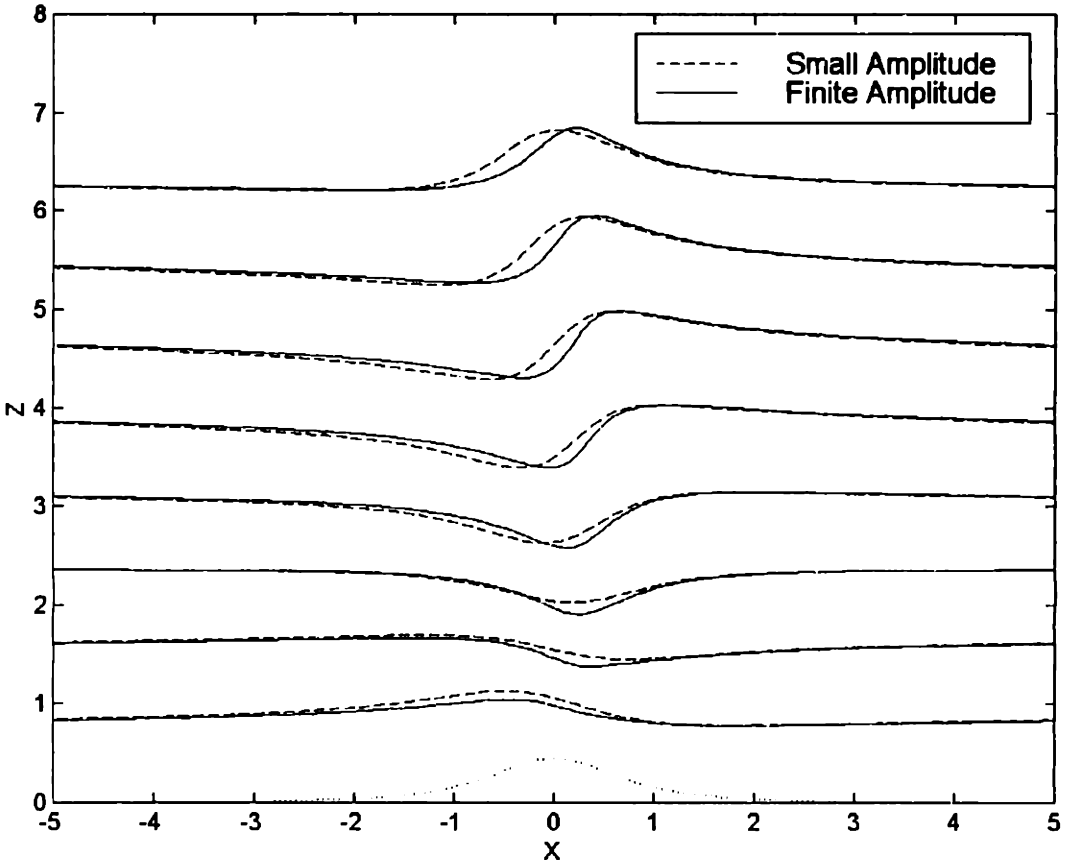


Figure 2.4: Streamlines for variable stratification.

### 2.5.2 Tropopause Tuning

For the situation of a higher value of $N$ above, a properly located discontinuity in stratification can cause an otherwise larger amplitude response, or tuning effect. This tuning effect is due to the amplification of the mountain waves by partial reflections off the tropopause. The small-amplitude response is tuned or maximized when the interface is at odd half multiples of the lower wavelength. In addition, the small-amplitude response is detuned or minimized when the interface is at multiples of the lower wavelength (Klemp and Lilly 1975). However, there is no precise criterion for the finite-amplitude response. For the solutions presented in this section, a variable stratification profile is used to approximate the two-layer solution. This substitution is due partly because of the convergence problems associated with the two-layer solution and partly to compare results when the interface is continuously varying.

In Figure 2.5, a few streamlines are plotted for a situation in which the small-amplitude response is tuned. The stratification parameters are $a = 1$, $b = 1/3$, $c = 20$, and $d = 4.71$. These parameters put a sharp interface at a height of one half the lower wavelength. This interface is indicated by the upper dotted line in the figure. Note that for the finite-amplitude solution the interface is actually along a streamline that starts at this elevation. The lower dotted line is the topography. The amplitude is moderate with $\varepsilon = 0.75$, where $\varepsilon$ is based on $a$. The small-amplitude solution predicts an unphysical situation in which breaking has occurred. The finite-amplitude response is not tuned in this case. In contrast, Figure 2.6 indicates a situation in which the finite-amplitude response is tuned. In this figure, the parameters are as in Figure 2.5 except $d = 5.94$. The interface and the topography are again indicated by the upper and lower dotted lines. A higher interface, 0.63 times the lower wavelength (Durran 1992), is required for the finite-amplitude response to be tuned. This result is likely due to the nonlinearity inherent in the

finite-amplitude problem. Similar to the small-amplitude response, tuning can also occur for the finite-amplitude response at higher interface elevations such as 1.26 times the lower wavelength. However, these heights are often of little physical interest for applications such as the earth's atmosphere. As seen by Durran (1992), the tuned finite-amplitude response appears to have 'kinks' in the streamlines, possibly indicating stagnation points. Upon careful examination at high numerical resolution, the 'kinks' are in regions were the radius of curvature of the streamlines is large, and therefore do not appear to be true stagnation points.

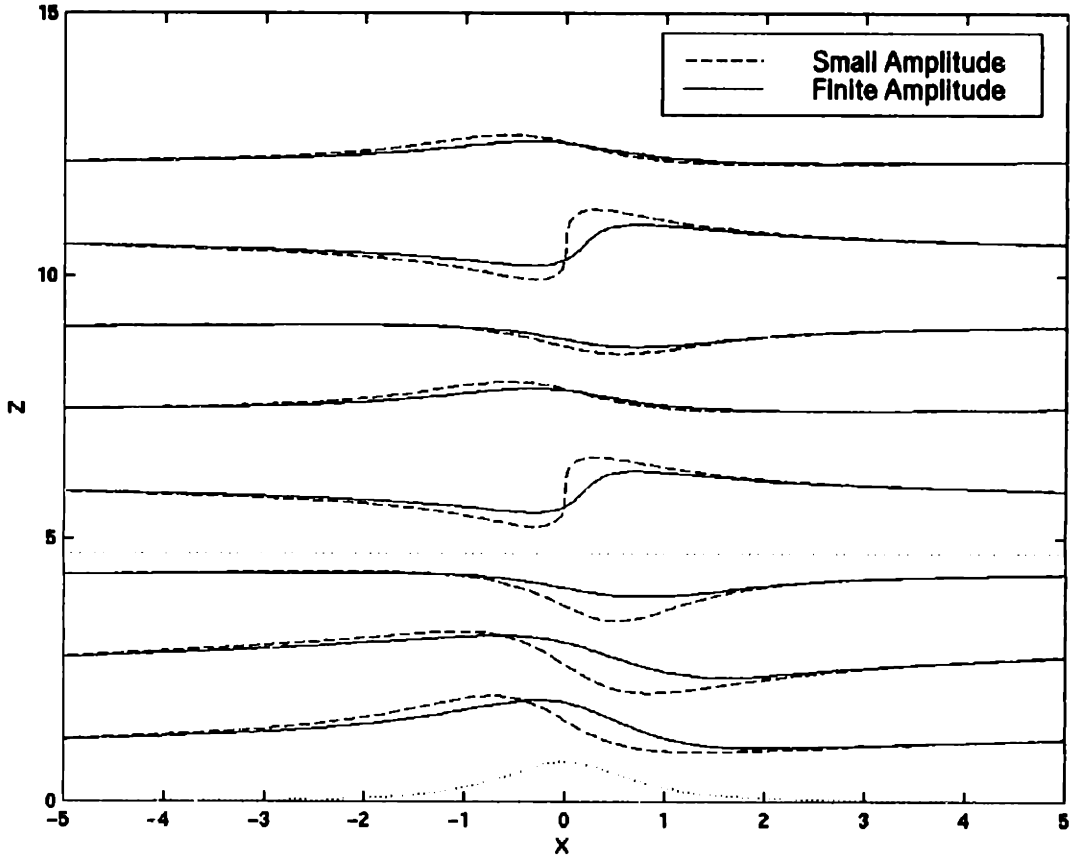


Figure 2.5: Streamlines for a sharp interface at $d = 4.71$.

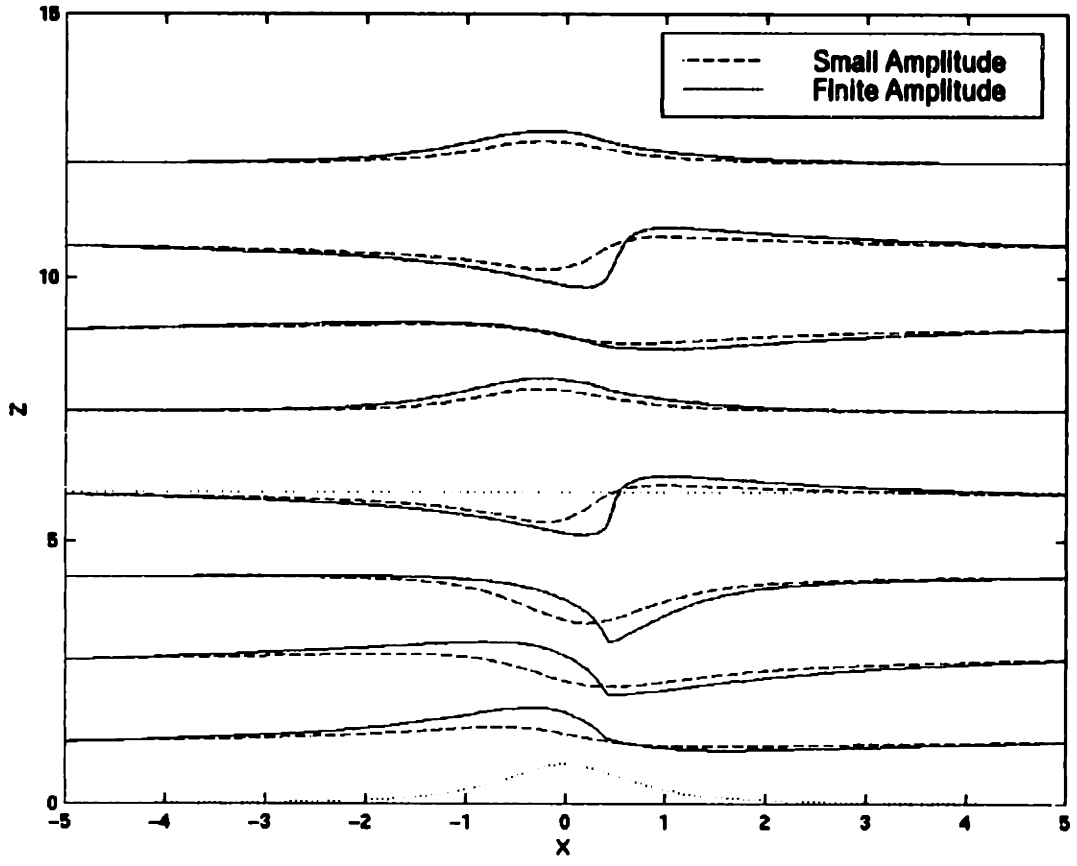


Figure 2.6: Streamlines for a sharp interface at $d = 5.94$.

The variable stratification allows the sharp discontinuity to continuously vary over a transition region. Figure 2.7 and Figure 2.8 correspond to Figure 2.5 and Figure 2.6, except that now $c = 2$. In both the small-amplitude and the finite-amplitude cases, the tuning effect is still present but is significantly diminished. For the finite-amplitude case, the profile curvature seems to have a more drastic effect. The streamline 'kinks' have vanished and the solution is reasonably close to the small-amplitude solution.

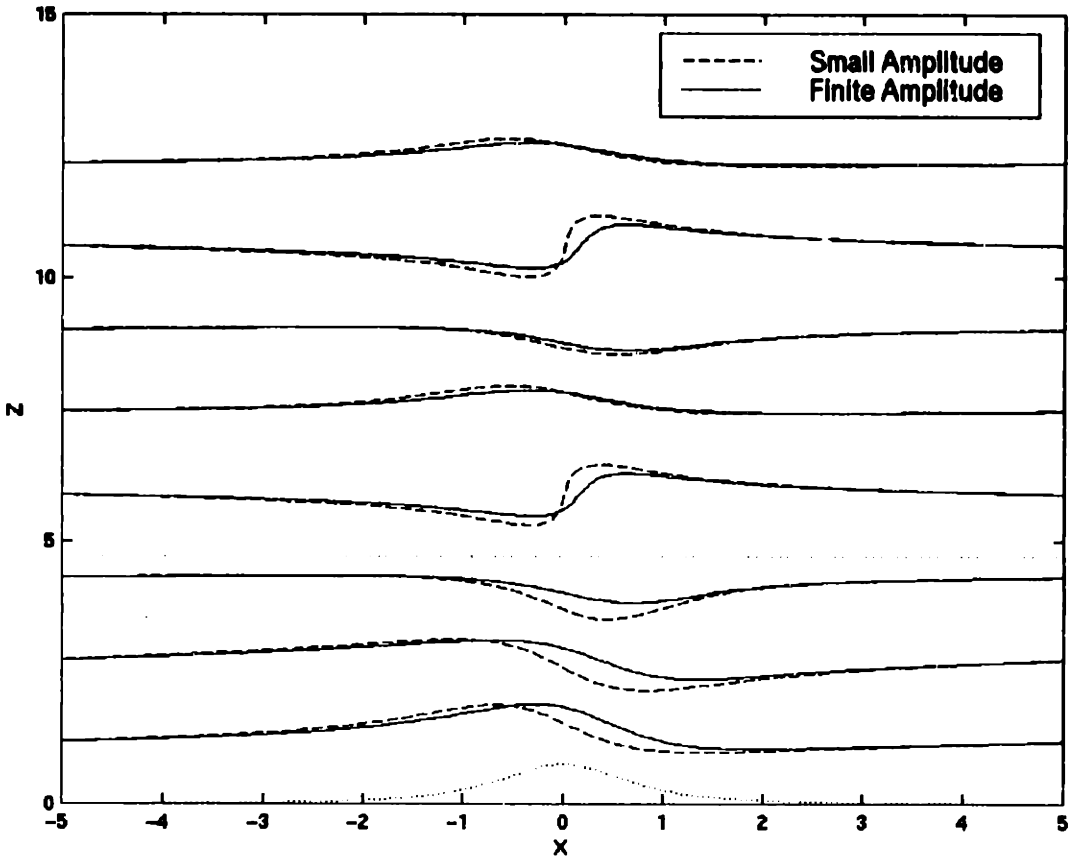


Figure 2.7: Streamlines for a continuously varying interface at $d = 4.71$.

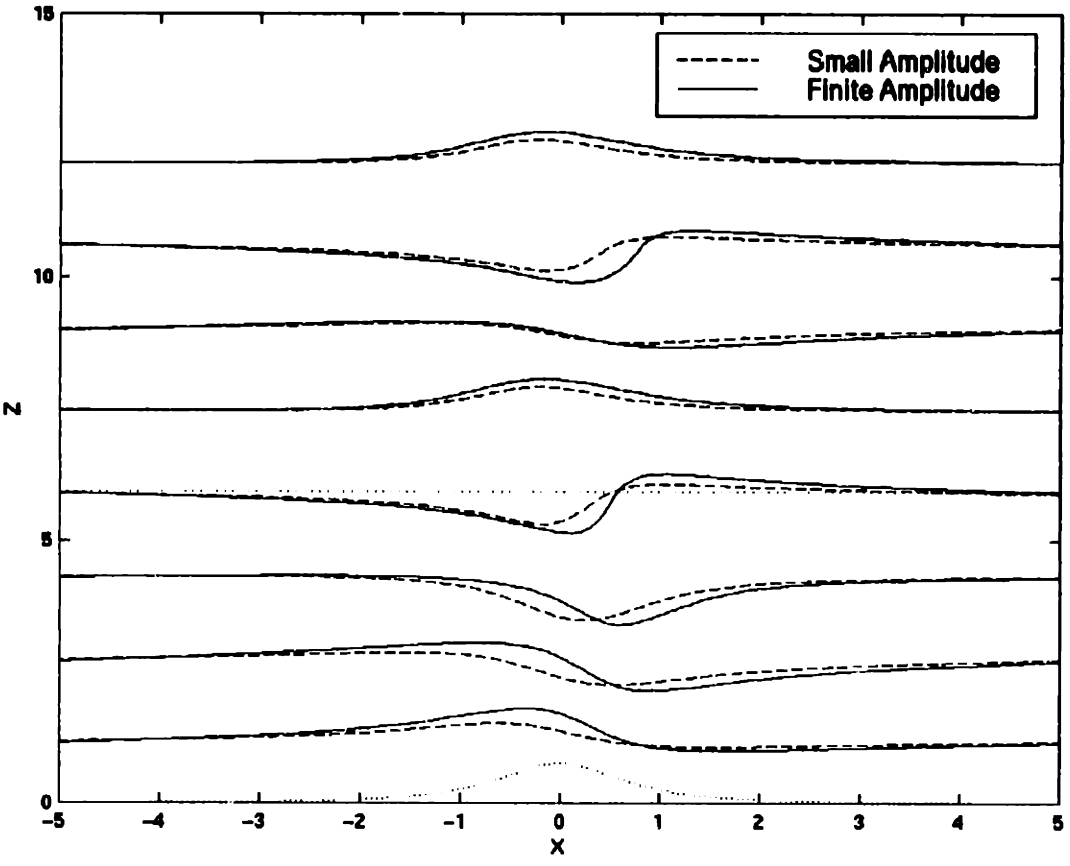


Figure 2.8: Streamlines for a continuously varying interface at $d = 5.94$.

# Chapter 3

# Three-Dimensional Flow

This chapter focuses on flow of a stratified fluid over three-dimensional topography of small-amplitude. Finite-amplitude topography introduces complicated nonlinear effects to the flow field, which are outside the scope of this thesis. However, three-dimensional topography allows for a more general representation of geophysical flows, e.g. a single mountain or a general arrangement of mountains in the Earth's atmosphere. In addition, the three-dimensional topography approximates the two-dimensional topography for long topography spanwise to the flow direction.

This chapter begins by presenting the three-dimensional analog of Long's equation. This equation is then reduced in the same fashion as the two-dimensional case. Next, the uniformly stratified solution is presented. Then, the solution for two layers of uniform stratification is presented. The final solution presented is for the general case of a single layer of variable stratification. A discussion of these solutions concludes the chapter. Included in this discussion are comments on the effect of tropopause tuning in the three-dimensional flow and a two-dimensional approximation of the three-dimensional flow.

## 3.1 General Formulation

Consider the flow of a steady, incompressible, and inviscid fluid in the absence of rotational effects. The governing equations are

$$\nabla \cdot \mathbf{u} = 0 \tag{3.1}$$

$$\mathbf{u} \cdot \nabla \rho = 0 \tag{3.2}$$

$$\rho \mathbf{u} \cdot \nabla \mathbf{u} = -\nabla p + \rho \mathbf{g} \tag{3.3}$$

As in Chapter 2, $\rho$ is the local fluid density, $\mathbf{u}$ is the local velocity vector, $p$ is the local pressure, and $\mathbf{g}$ is the downward pointing gravitational acceleration. Equations 3.1 – 3.3 respectively represent incompressibility, mass balance, and momentum balance. In this chapter, the coordinate system is such that the $x$-direction is horizontal, the $y$-direction is spanwise to the incipient flow, and the $z$-direction is vertical. Note that Equation 3.2 indicates that $\mathbf{u}$ is orthogonal to $\nabla\rho$, i.e. $\mathbf{u}$ lies in surfaces of constant $\rho$. Before proceeding further, two stream functions, $\Psi$ and $\Phi$, are introduced as follows,

$$\mathbf{u} = \nabla\Psi \times \nabla\Phi \,. \tag{3.4}$$

Introducing these two streamfunctions automatically satisfies Equation 3.1. In addition, the vorticity, $\varpi$, is introduced as

$$\varpi = \nabla \times \mathbf{u} \,. \tag{3.5}$$

Also, the assumption of no upstream influence is invoked to give the following upstream flow conditions,

$$\mathbf{u} = U_0 \hat{i} \,, \tag{3.6}$$

$$\rho = \rho_0(z). \tag{3.7}$$

These upstream conditions are in terms of the uniform free-stream velocity, $U_0$, and the characteristic free-stream density, $\rho_0$. These conditions can be recast using the streamfunctions,

$$\Psi = U_0 z \,, \tag{3.8}$$

$$\Phi = y \,, \tag{3.9}$$

$$\rho = \rho_0\left(\frac{\Psi}{U_0}\right). \tag{3.10}$$

Therefore, Equation 3.3 becomes

$$\rho(\varpi \times \mathbf{u}) = -\nabla\left(p + \frac{1}{2}\rho|\mathbf{u}|^2 + \rho g z\right) + \nabla\rho\left(\frac{1}{2}|\mathbf{u}|^2 + gz\right). \tag{3.11}$$

This equation can be further simplified by expanding the left side as

$$\varpi \times \mathbf{u} = \varpi \times (\nabla\Phi \times \nabla\Psi) = (\varpi \cdot \nabla\Psi)\nabla\Phi - (\varpi \cdot \nabla\Phi)\nabla\Psi. \tag{3.12}$$

Invoking the Vorticity Theorem, which states that the vortex lines for a stratified flow started from rest are on surfaces of constant density (Yih 1980, p. 14), allows for further simplification of Equation 3.12. Assuming the steady state flow under discussion evolved from a flow at rest, the Vorticity Theorem can be written symbolically for this situation as

$$\varpi \cdot \nabla\rho = 0. \tag{3.13}$$

A detailed derivation of Equation 3.13 is also given in Appendix A. Since $\nabla\rho$ is parallel to $\nabla\Psi$ from Equation 3.10, this condition can be written as

$$\varpi \cdot \nabla\Psi = 0. \tag{3.14}$$

Therefore, the first term on the right side of Equation 3.12 is zero. After eliminating this term and substituting for $\nabla\rho$, Equation 3.11 becomes

$$\rho(\varpi \cdot \nabla\Phi)\nabla\Psi = \nabla\left(p + \frac{1}{2}\rho|\mathbf{u}|^2 + \rho g z\right) - \left(\frac{1}{2}|\mathbf{u}|^2 + gz\right)\frac{d\rho}{d\Psi}\nabla\Psi. \tag{3.15}$$

Imposing the upstream conditions from above gives

$$\varpi \cdot \nabla\Phi = \frac{1}{\rho}\frac{d\rho}{d\Psi}\left[\frac{1}{2}U_0^2 - \frac{1}{2}|\mathbf{u}|^2 + \frac{g}{U_0}(\Psi - U_0 z)\right]. \tag{3.16}$$

Scaling in accordance with the two-dimensional case, the following substitutions are made,

$$x = L\tilde{x},\ \ y = L\tilde{y},\ \ z = \frac{U_0}{N_0}\tilde{z},\ \ u = U_0\tilde{u},\ \ v = U_0\tilde{v},\ \ w = \frac{U_0^2}{LN_0}\tilde{w},$$

$$\rho = \rho_0\tilde{\rho},\ \ p = \frac{gU_0\rho_0}{N_0}\tilde{p},\ \ \Psi = \frac{U_0^2}{N_0}\tilde{\Psi},\ \ \Phi = L\tilde{\Phi}. \tag{3.17}$$

In this substitution, $L$ represents a characteristic length scale such as the topography half-width, $N_0$ represents a characteristic Brunt-Väisälä frequency, and $U_0$ and $\rho_0$ represent the characteristic free-stream quantities as before. In making these substitutions, two dimensionless parameters arise, $\beta$ and $\mu$. These parameters are defined as

$$\beta = \frac{N_0 U_0}{g}, \quad \mu = \frac{U_0}{N_0 L}. \tag{3.18}$$

The first parameter is called the Boussinesq parameter and controls stratification effects. The second parameter is called the longwave parameter and controls dispersive effects. As in the two-dimensional case, both of these parameters are assumed to be small. After making these assumptions, the dimensionless form of Equation 3.16 and Equation 3.14 respectively become

$$\varpi_H \cdot \nabla\Phi + N^2(\Psi)(\Psi - z) = 0, \tag{3.19}$$

$$\varpi_H \cdot \nabla\Psi = 0. \tag{3.20}$$

Because of the scaling and the hydrostatic assumption, a hydrostatic vorticity appears in the above equations, which is defined as

$$\varpi_H = \left( -\frac{\partial v}{\partial z}, \frac{\partial u}{\partial z}, \frac{\partial v}{\partial x} - \frac{\partial u}{\partial y} \right). \tag{3.21}$$

As a check, consider the two-dimensional limit of Equation 3.19 and Equation 3.20. In this limit, $\Phi = y$, $u = \Psi_z$, $w = -\Psi_x$, and the hydrostatic vorticity reduces to

$$\varpi_H = \left( 0, \frac{\partial u}{\partial z}, 0 \right). \tag{3.22}$$

Therefore Equation 3.20 is automatically satisfied and Equation 3.19 becomes

$$\Psi_{zz} + N^2(\Psi)(\Psi - z) = 0. \tag{3.23}$$

Equation 3.23 exactly agrees with the two-dimensional result given in Equation 2.30. Equation 3.19 can be written more conveniently by introducing the streamline perturbations, $\psi$ and $\phi$, via the following definitions,

$$\Psi = \psi + z, \tag{3.24}$$

$$\Phi = \phi + y. \tag{3.25}$$

Substituting in Equation 3.19 and Equation 3.20 and retaining only the linear terms gives

$$\psi_{zz} + N^2(z)\psi + \phi_{yz} = 0, \tag{3.26}$$

$$\phi_{xx} + \phi_{yy} + \psi_{yz} = 0. \tag{3.27}$$

Eliminating $\phi$ between these two equations yields a single linear equation for $\psi$,

$$\psi_{xxzz} + N^2(z)(\psi_{xx} + \psi_{yy}) = 0. \tag{3.28}$$

Solutions to this equation depend upon the profile of the stratification as indicated by the appearance of $N(z)$.

In addition, two boundary conditions must be satisfied. First, there is no normal flow on the surface of the topography. Since the topography is a stream surface and $\Psi$ is constant on the topography far upstream or downstream, the lower boundary condition can be written as

$$\Psi(x, y, f) = const. \tag{3.29}$$

The constant can be chosen to be zero without loss of generality. In this chapter, the topography used is given by

$$f(x,y) = \frac{h}{\left[1 + \left(\frac{x}{L_x}\right)^2 + \left(\frac{y}{L_y}\right)^2\right]^{3/2}}. \tag{3.30}$$

The parameters, $L_x$ and $L_y$, determine the three-dimensionality of the topography. The 3/2 exponent in the denominator prevents the topography from having infinite volume and vertical cross-sections with infinite area. Scaling Equation 3.29 as before and scaling $f(x)$ by $h$ gives

$$\Psi(x, y, \varepsilon f) = 0. \tag{3.31}$$

The resulting dimensionless parameter, $\varepsilon$, is defined as

$$\varepsilon = \frac{hN_0}{U_0}. \tag{3.32}$$

This parameter effectively controls the amplitude of the response. Introducing the streamline perturbation, $\psi$, then gives

$$\psi(x, y, \varepsilon f) = -\varepsilon f. \tag{3.33}$$

Since Equation 3.28 has been linearized, the equation is valid only for the small-amplitude case. Thus, the boundary condition can be applied at $z = 0$ instead of on the actual topography. As $\varepsilon \to 0$, this boundary condition reduces to

$$\psi(x, y, 0) = -\varepsilon f. \tag{3.34}$$

The second boundary condition is satisfied as $z \to \infty$. Since the flow is steady, energy from the topography must be radiated outwards. This type of boundary condition is often referred to as the radiation condition. This condition is met by insuring that the vertical group velocity is positive. Defining $k$ as the horizontal wavenumber associated with the $x$-direction, $l$ as the spanwise wavenumber associated with the $y$-direction, and $m$ as the vertical wavenumber associated with the $z$-direction, the dispersion relation for hydrostatic flow is given by (Baines 1995, p. 356)

$$\omega(k, l, m) = k - \frac{\mathrm{sgn}(k)\,\mathrm{sgn}(m) N \sqrt{k^2 + l^2}}{m}. \tag{3.35}$$

As a check, the two-dimensional limit of Equation 3.35, as $l \to 0$, agrees with Equation 2.41. The vertical group velocity is then given by

$$c_g\big|_z = \frac{\partial \omega}{\partial m} = \frac{\mathrm{sgn}(k)\mathrm{sgn}(m)N\sqrt{k^2+l^2}}{m^2}. \tag{3.36}$$

For the vertical group velocity to be positive,

$$km > 0. \tag{3.37}$$

Application of the radiation condition is further developed specifically for the uniform stratification case in Section 3.2.

As mentioned above, the solution depends upon the profile of the stratification. In Section 3.2, a single uniformly stratified layer is examined. This solution is extended in Section 3.3 for two layers of uniform stratification and extended further in Section 3.4 to variable stratification.

## 3.2 Single Layer of Uniform Stratification

The simplest stratification profile is a single semi-infinite layer of uniform stratification, i.e. $N(z) = N$. For this situation, solutions to Equation 3.28 can be written in double Fourier integral form,

$$\psi(x,y,z) = \int_{-\infty}^{\infty}\int_{-\infty}^{\infty} \hat{\psi}(k,l,z)e^{i(kx+ly)}dkdl. \tag{3.38}$$

The streamline perturbation in the wavenumber domain in turn satisfies

$$\hat{\psi}_{zz} + m^2\hat{\psi} = 0. \tag{3.39}$$

The vertical wavenumber, $m$, is defined as

$$m = N\frac{\sqrt{k^2+l^2}}{k}. \tag{3.40}$$

Solutions to Equation 3.39 take the form

$$\hat{\psi} = Ae^{imz} + Be^{-imz}. \tag{3.41}$$

Therefore, the solution to Equation 3.28 can be written as

$$\psi(x,y,z) = \int_{-\infty}^{\infty}\int_{-\infty}^{\infty}\left(Ae^{imz} + Be^{-imz}\right)e^{i(kx+ly)}dkdl. \tag{3.42}$$

The functions, $A(k,l)$ and $B(k,l)$, are determined by applying the radiation condition and the lower boundary condition.

To impose the radiation condition, terms with a negative vertical group velocity must be suppressed. In view of Equation 3.37 and Equation 3.40, the radiation condition is satisfied by setting $B(k,l) = 0$.

The remaining function, $A(k,l)$, is determined by imposing the lower boundary condition. Converting Equation 3.34 into the wavenumber domain gives

$$\hat{\psi}(k,l,0) = -\varepsilon\hat{f}(k,l). \tag{3.43}$$

Substituting in Equation 3.41 gives

$$A(k,l) = -\varepsilon\hat{f}(k,l). \tag{3.44}$$

The solution for the single layer of uniform stratification can thus be formally written as

$$\psi(x,y,z) = \int_{-\infty}^{\infty}\int_{-\infty}^{\infty} -\varepsilon\hat{f}e^{i(kx+ly+mz)}dkdl. \tag{3.45}$$

Numerically, this integral can be easily discretized into a linear system.

## 3.3 Two Layers of Uniform Stratification

Now consider a layer of finite height with uniform stratification, $N(z) = N_L$, above which is a semi-infinite layer with uniform stratification, $N(z) = N_U$. Even though the

governing equations have been linearized, a tuning effect is expected for this stratification profile as suggest by the small-amplitude two-dimensional solution.

The governing equations presented in Section 3.1 are valid in each layer. Further, the solution in each layer will take the form presented in Section 3.2. Since the governing equations are only valid for small-amplitude solutions, the interface is at a constant height, $z^*$. The solution can thus be constructed in a piecewise fashion,

$$\hat{\psi}_L = Ae^{im_L z} + Be^{-im_L z} \quad \text{for} \quad 0 < z < z^*, \tag{3.46}$$

$$\hat{\psi}_U = Ce^{im_U (z-z^*)} + De^{-im_U (z-z^*)} \quad \text{for} \quad z > z^*. \tag{3.47}$$

Note that there is a different vertical wavenumber, $m_L$ and $m_U$, for each layer, which in turn correspond to the different stratification constants, $N_L$ and $N_U$, through the relation given in Equation 3.40. To determine $A$, $B$, $C$, and $D$, a total of four boundary conditions are needed. First, the radiation condition must be satisfied as $z \to \infty$. Suppressing the terms with negative vertical group velocity in the upper layer gives

$$D(k,l) = 0. \tag{3.48}$$

Next, there are two matching conditions at $z = z^*$,

$$\hat{\psi}_L(k,l,z^*) = \hat{\psi}_U(k,l,z^*), \tag{3.49}$$

$$\frac{\partial \hat{\psi}_L}{\partial z}(k,l,z^*) = \frac{\partial \hat{\psi}_U}{\partial z}(k,l,z^*). \tag{3.50}$$

After the appropriate differentiation and substitution, these matching conditions become

$$Ae^{im_L z^*} + Be^{im_L z^*} = C, \tag{3.51}$$

$$im_L Ae^{im_L z^*} + im_L Be^{im_L z^*} = im_U C. \tag{3.52}$$

Finally, the lower boundary condition from Equation 3.34 gives

$$A(k,l) + B(k,l) = -\varepsilon \hat{f}(k,l). \tag{3.53}$$

Thus there are four equations, Equations 3.48, 3.51, 3.52, and 3.53, to solve for the four unknowns, $A$, $B$, $C$, and $D$. Solving for these unknowns gives

$$A(k,l)=\frac{-\left(\frac{m_L}{m_U}+1\right)e^{-im_L z^*}}{\left(\frac{m_L}{m_U}-1\right)e^{im_L z^*}+\left(\frac{m_L}{m_U}+1\right)e^{-im_L z^*}}\varepsilon\hat{f}\,, \tag{3.54}$$

$$B(k,l)=\frac{-\left(\frac{m_L}{m_U}-1\right)e^{im_L z^*}}{\left(\frac{m_L}{m_U}-1\right)e^{im_L z^*}+\left(\frac{m_L}{m_U}+1\right)e^{-im_L z^*}}\varepsilon\hat{f}\,, \tag{3.55}$$

$$C(k,l)=\frac{-2\frac{m_L}{m_U}}{\left(\frac{m_L}{m_U}-1\right)e^{im_L z^*}+\left(\frac{m_L}{m_U}+1\right)e^{-im_L z^*}}\varepsilon\hat{f}\,, \tag{3.56}$$

$$D(k,l)=0. \tag{3.57}$$

Therefore the solutions to Equations 3.46 and 3.47 are known in the wavenumber domain for both layers. The solution in the real domain is found by applying Equation 3.38 to both layers.

Numerically, the integrals involved in the above solution can be easily discretized into a linear system. Moreover, since the solution is for the small-amplitude case, no iteration is required.

## 3.4 Variable Stratification

Now consider stratification that varies with height, i.e. $N=N(z)$. This situation accommodates general stratification profiles as well as three-dimensional effects, however the solution is limited to the small-amplitude case. As in the two-dimensional case, a hyperbolic tangent profile is used,

$$N(z) = a + b\tanh[c(z-d)]. \tag{3.58}$$

The parameters, $a$, $b$, $c$, and $d$, are used simply to adjust the size, shape, and location of the profile. Other functions can be used, but this function allows for the approximation of the two-layer solution.

Since the governing equation is still linear for this case, the solution can again be written using a double Fourier integral as in Equation 3.38. Further, the streamline perturbation in the wavenumber domain satisfies Equation 3.39. However, in this case the coefficients are not only parametric in $k$ and $l$, but also variable in $z$. This can be observed through the relationship

$$m(z) = N(z)\frac{\sqrt{k^2+l^2}}{k}. \tag{3.59}$$

The solution can then be posed using separation of variables. Introducing $\eta_1(z)$ and $\eta_2(z)$ yields a solution of the form

$$\hat{\psi}(k,l,z) = A(k,l)\eta_1(z) + B(k,l)\eta_2(z). \tag{3.60}$$

Therefore, $\eta_1(z)$ and $\eta_2(z)$ are independent solutions of

$$\frac{d\eta(z)}{dz} + m^2(z)\eta(z) = 0. \tag{3.61}$$

Note that $\eta_1(z)$ and $\eta_2(z)$ still parametrically depend on $k$ and $l$. Choosing the following 'initial' conditions for $\eta_1(z)$ and $\eta_2(z)$ automatically satisfies the lower boundary condition,

$$\eta_1(0) = 1,\ \eta_2(0) = 0,\ \frac{d\eta_1}{dz}(0) = 0,\ \frac{d\eta_2}{dz}(0) = 1. \tag{3.62}$$

This formulation effectively determines $A(k,l)$ as

$$A(k,l) = -\varepsilon\hat{f}(k,l). \tag{3.63}$$

Next, $\eta_1(z)$ and $\eta_2(z)$ can be found by 'shooting' to the top of the numerical domain. For the solutions presented in Section 3.5, a fourth-order Runge-Kutta scheme is used. Applying the

radiation condition will yield the remaining unknown $B(k,l)$. However, the stratification varies in $z$ and the technique developed in Section 2.4 must be employed to apply the radiation condition. A fictitious upper layer with uniform stratification, $N = N_\infty$, can be introduced at the top of the computational domain, $z = z_\infty$. Note that $z_\infty$ must be sufficiently high such that $N(z)$ has asymptotically approached a constant. In the fictitious layer, the solution takes the usual form,

$$\hat{\psi}_\infty = Ce^{im_\infty(z-z_\infty)} + De^{-im_\infty(z-z_\infty)}. \tag{3.64}$$

In this fictitious layer, the radiation condition is simply

$$D(k,l) = 0. \tag{3.65}$$

In addition, there are two matching conditions,

$$\hat{\psi}(k,l,z_\infty) = \hat{\psi}_\infty(k,l,z_\infty), \tag{3.66}$$

$$\frac{\partial\hat{\psi}}{\partial z}(k,l,z_\infty) = \frac{\partial\hat{\psi}_\infty}{\partial z}(k,l,z_\infty). \tag{3.67}$$

In turn, these matching conditions yield,

$$A\eta_1(z_\infty) + B\eta_2(z_\infty) = C, \tag{3.68}$$

$$A\frac{d\eta_1}{dz}(z_\infty) + B\frac{d\eta_2}{dz}(z_\infty) = im_\infty C. \tag{3.69}$$

Thus there are four equations, Equations 3.63, 3.65, 3.68, and 3.69, to solve for the four unknowns, $A$, $B$, $C$, and $D$. Solving for the remaining unknown of interest, $B(k,l)$, gives

$$B(k,l) = \frac{\frac{d\eta_1}{dz}(z_\infty) - im_\infty\eta_1(z_\infty)}{\frac{d\eta_2}{dz}(z_\infty) - im_\infty\eta_2(z_\infty)}\hat{\varepsilon f}. \tag{3.70}$$

Therefore the solution to Equation 3.39 is known in the wavenumber domain. The solution in the real domain is found by applying Equation 3.38.

Numerically, the integrals involved in the above solution can be easily discretized into a linear system. Again, since the solution is for the small-amplitude case, no iteration is required.

## 3.5 Discussion

For the purposes of this discussion, the topography used is of the form in Equation 3.30. In addition, the variable stratification profile used is of the form in Equation 3.58. All of the figures shown in this section are in dimensionless form.

Since the streamfunction, $\Psi$, is a function of $x$, $y$, and $z$ for the three-dimensional case, the streamfunction is difficult to plot in a concise manner. One possibility is to plot the value of the streamfunction for a few particular heights in the flow field. In Figure 3.1, the value of the streamfunction for $z = 0$ and $z = \pi/2$ is plotted as a function of $x$ and $y$ for a uniformly stratified flow, $N = 1$. The mountain aspect ratio, $L_x/L_y$, is 1/2 and $\varepsilon = 0.75$. These flow parameters are the same as for Figure 2.2 except the mountain is now three-dimensional. This depiction of the flow field does not lend itself to easy comparison with the two-dimensional examples in Chapter 2. Since the mountain is symmetric about the $y = 0$ plane, the streamlines in the $y = 0$ plane can be used to represent the entire flow field. In Figure 3.2, the center-plane streamlines are plotted for the same flow situation and topography as Figure 3.1. The lower dotted line in the figure represents the topography. In this form, the three-dimensional flow can be easily compared to the equivalent two-dimensional flow in Figure 2.2. Note that the streamline perturbations above the mountain have been reduced for the three-dimensional case. Since the flow is no longer constrained to only pass over the mountain and can now go around the mountain as well, this result agrees with physical intuition.

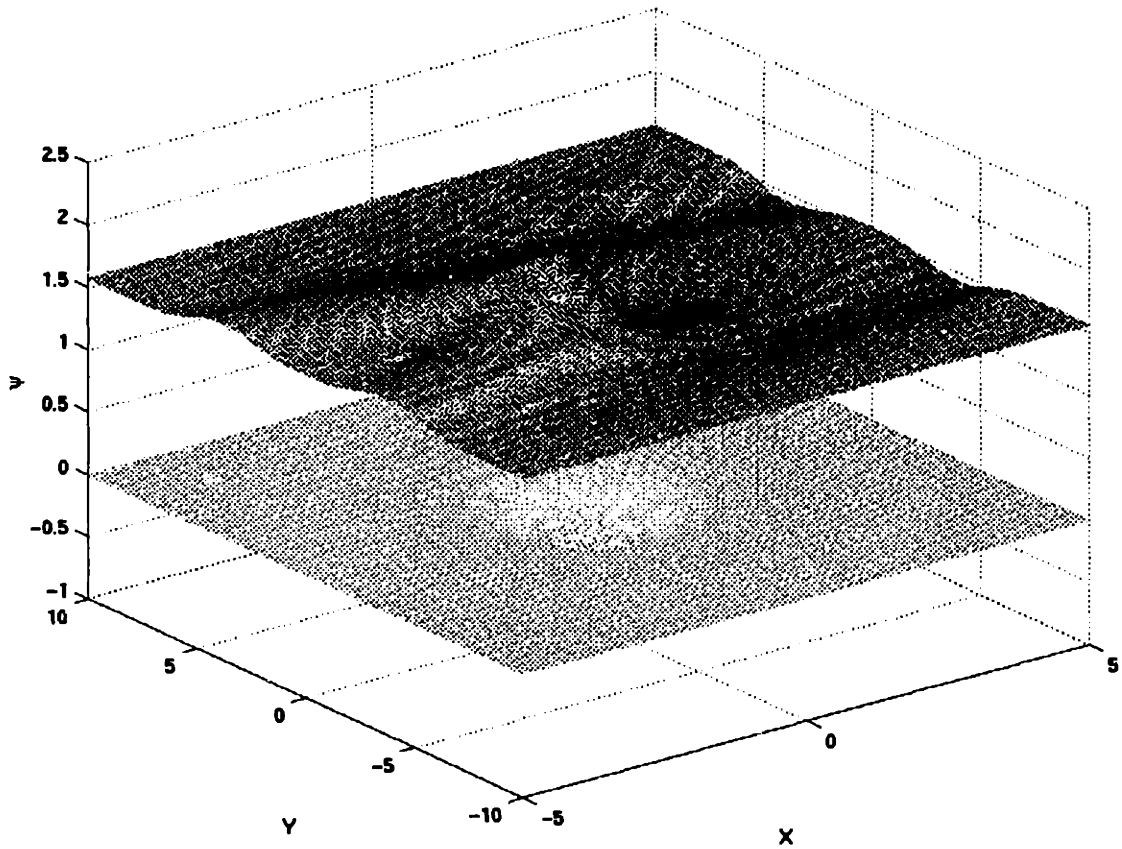


Figure 3.1: Streamfunction for a single layer of uniform stratification.

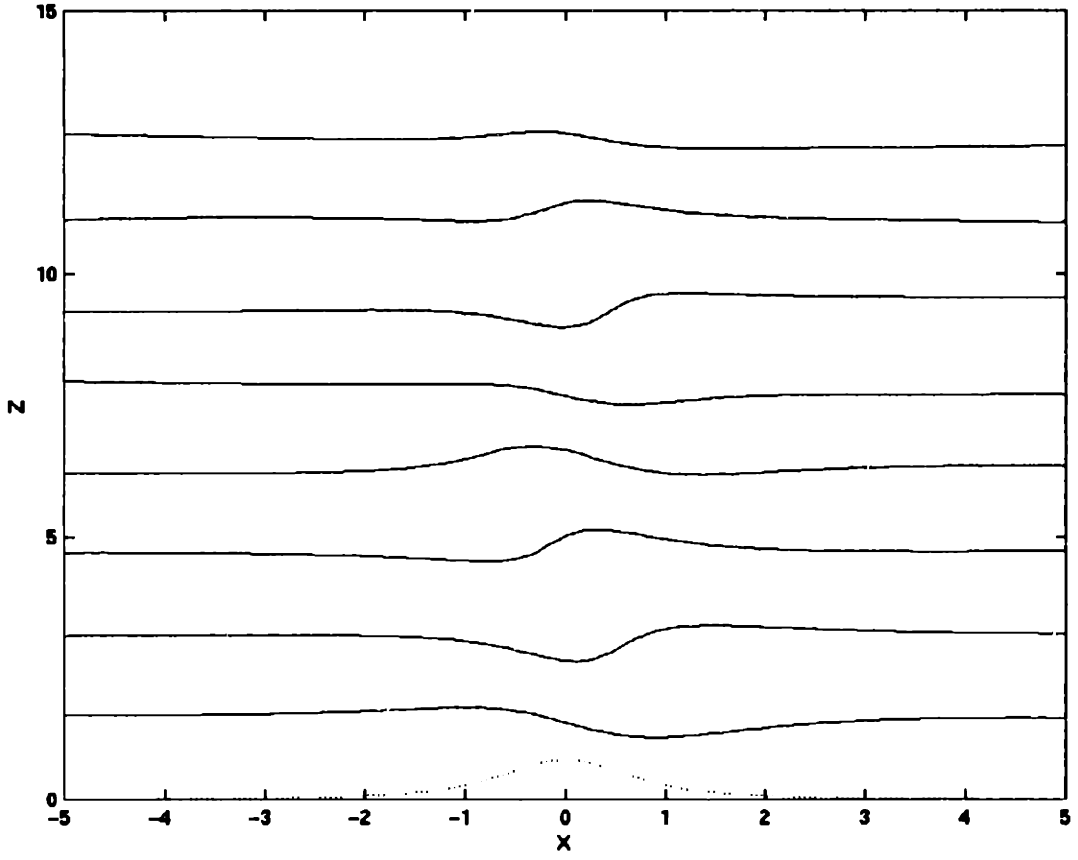


Figure 3.2: Center-plane streamlines for a single layer of uniform stratification.

The center plane representation, as depicted in Figure 3.2, is particularly convenient for Section 3.5.1 in discussing the effect of three-dimensionality on tropopause tuning. However, the surface plots, as depicted in Figure 3.1, are useful in presenting the two-dimensional approximation in Section 3.5.2.

### 3.5.1 Tropopause Tuning

As shown in Section 2.5.2, for the case of a higher value of $N$ above, a properly located discontinuity in the stratification structure can cause a tuning effect. For the three-dimensional

case, only the small-amplitude tuning effects can be discussed. For the solutions presented in this section, a variable stratification profile is used to approximate the two-layer profile. This substitution is for consistency with the two-dimensional case in Section 2.5.2 and to compare results when the interface is continuously varying.

In Figure 3.3, a few center-plane streamlines are plotted for a situation in which the three-dimensional response is tuned. This situation is identical to the situation in which the two-dimensional small-amplitude response is tuned in Figure 2.5. The stratification parameters are $a = 1$, $b = 1/3$, $c = 20$, and $d = 4.71$. These parameters put a sharp interface at a height of one half the lower wavelength. This interface is indicated by the upper dotted line in the figure. The lower dotted line indicates the topography. The amplitude, which is based on $a$, is $\varepsilon = 0.75$. The dashed streamlines represent the solution for a mountain with an aspect ratio of 1/16, and the solid streamlines represent the solution for a mountain with an aspect ratio of 1/2. The former closely approximates the small-amplitude two-dimensional solution from Figure 2.5, again indicating an unphysical situation in which breaking is occurring. However, the tuning effect, while still present, is reduced for the largely three-dimensional mountain.

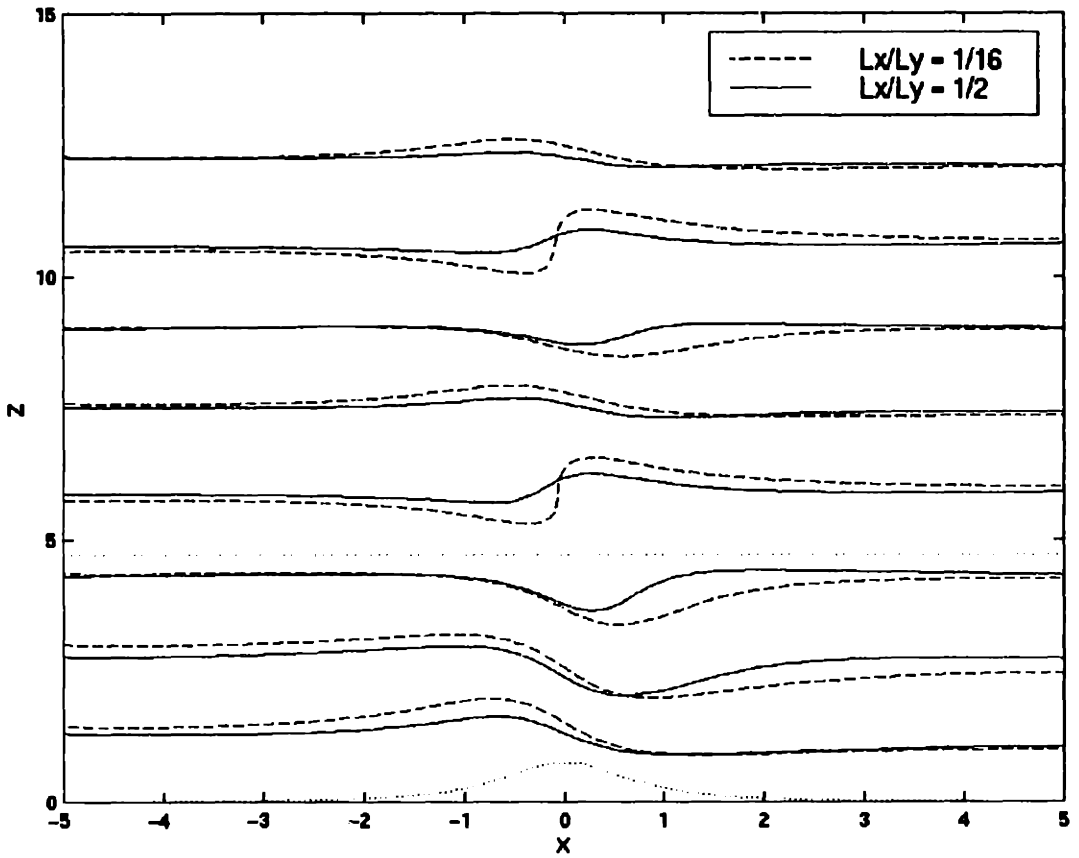


Figure 3.3: Center-plane streamlines for a sharp interface at $d = 4.71$.

In Figure 3.4, a few center-plane streamlines are plotted for a continuously varying stratification profile. The stratification parameters are the same as Figure 3.3 except that now $c = 2$. Again, the upper and lower dotted lines respectively represent the interface and the topography. In addition, the solution is plotted for two different aspect ratios as indicated in the figure. When $L_x / L_y = 1/16$, the solution closely approximates the small-amplitude two-dimensional solution from Figure 2.6. For the largely three-dimensional mountain, the tuning effect is diminished because of two factors, the continuously varying stratification profile and the three-dimensionality.

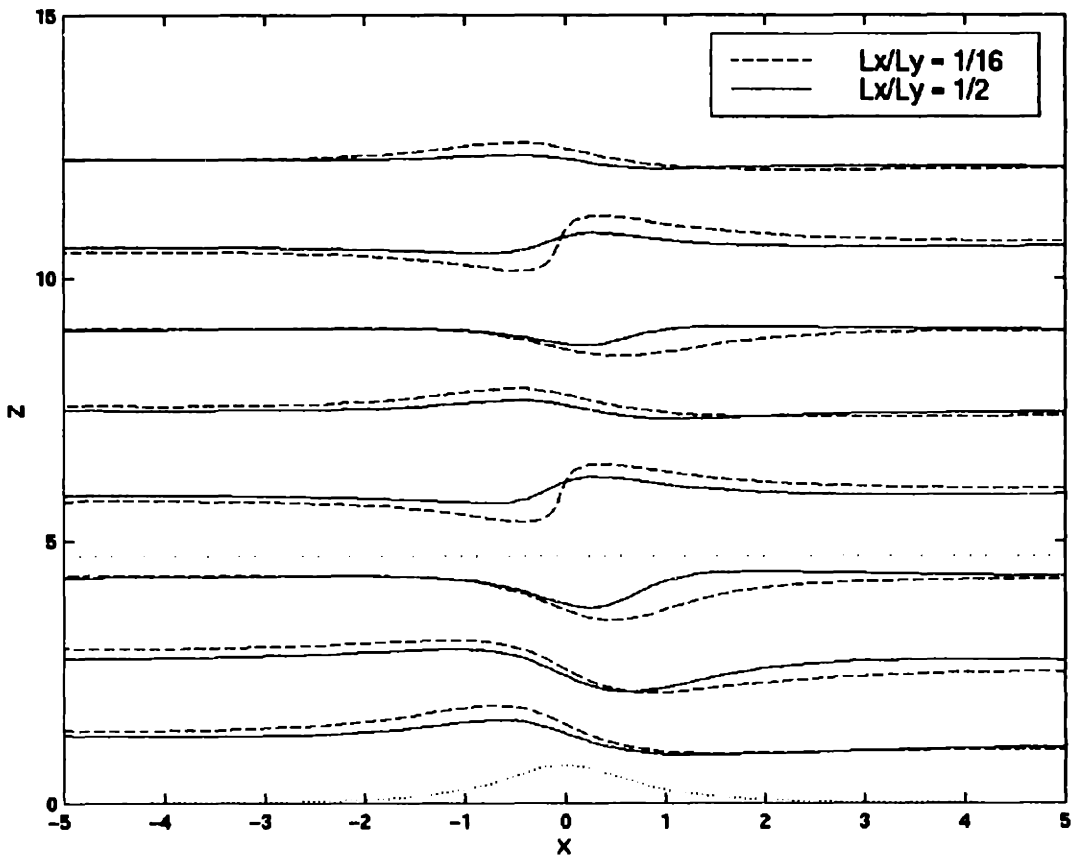


Figure 3.4: Center-plane streamlines for a continuously varying interface at $d = 4.71$.

### 3.5.2 Two-Dimensional Approximation

As indicated in Figures 3.3 and 3.4, the three-dimensional solution approximates the small-amplitude solution for topography with a small aspect ratio, i.e. $L_x / L_y << 1$. Thus, for a mountain that is slowly varying in the spanwise direction, the three-dimensional solution can be constructed by solving a series of two-dimensional problems spanwise across the topography.

In Figure 3.5, the value of the streamfunction, at $z = 0$ and $z = \pi/2$, is plotted for a three-dimensional solution constructed from two-dimensional solutions as described above. The flow situation is the same as the situation for Figure 3.1, in which the actual three-dimensional

solution is plotted. The topography for these two situations has an aspect ratio of 1/2. As expected, the two-dimensional approximation fails to capture the flow that is diverted around the mountain instead of over the mountain.

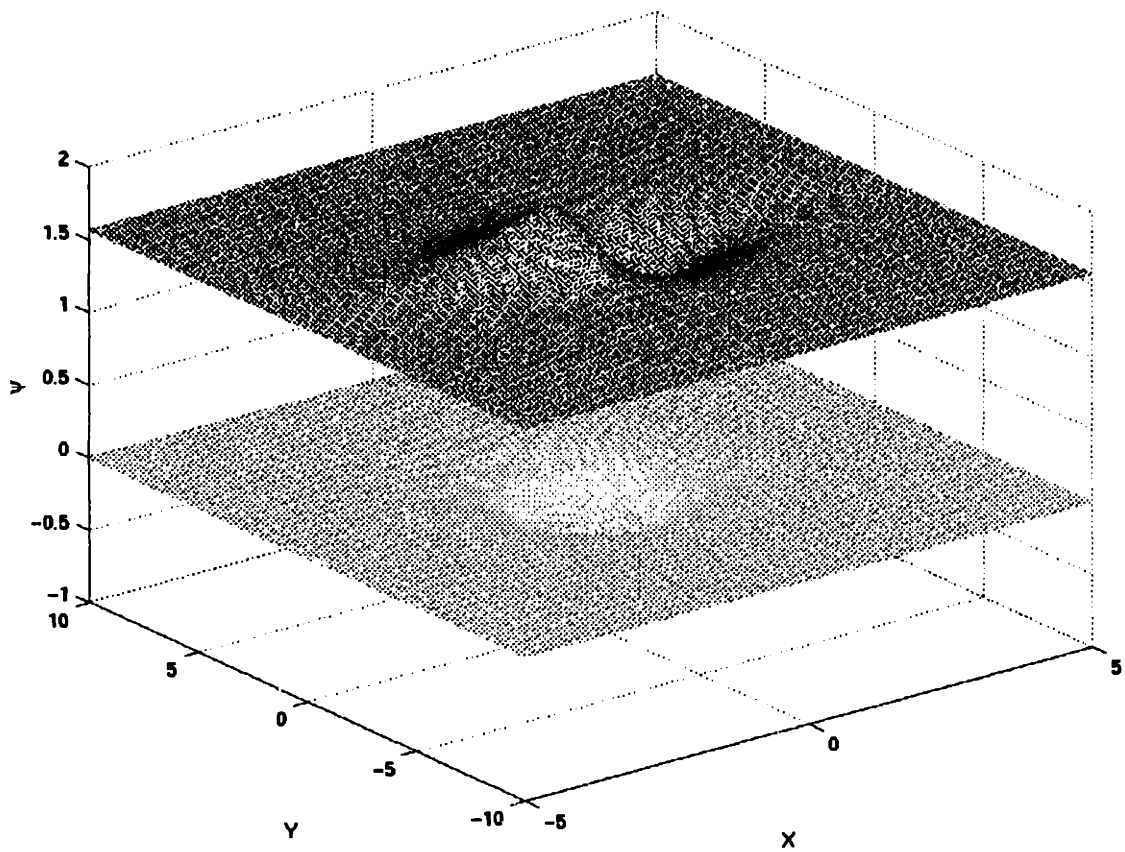


Figure 3.5: Streamfunction for two-dimensional approximation with $L_x / L_y = 1/2$.

In contrast, the actual and approximate solutions for an aspect ratio of 1/16 are respectively plotted in Figures 3.6 and 3.7. For this situation, the two-dimensional approximation is close to the actual three-dimensional solution. This result is because the mountain is long in the spanwise direction and hence very little flow is diverted around the mountain.

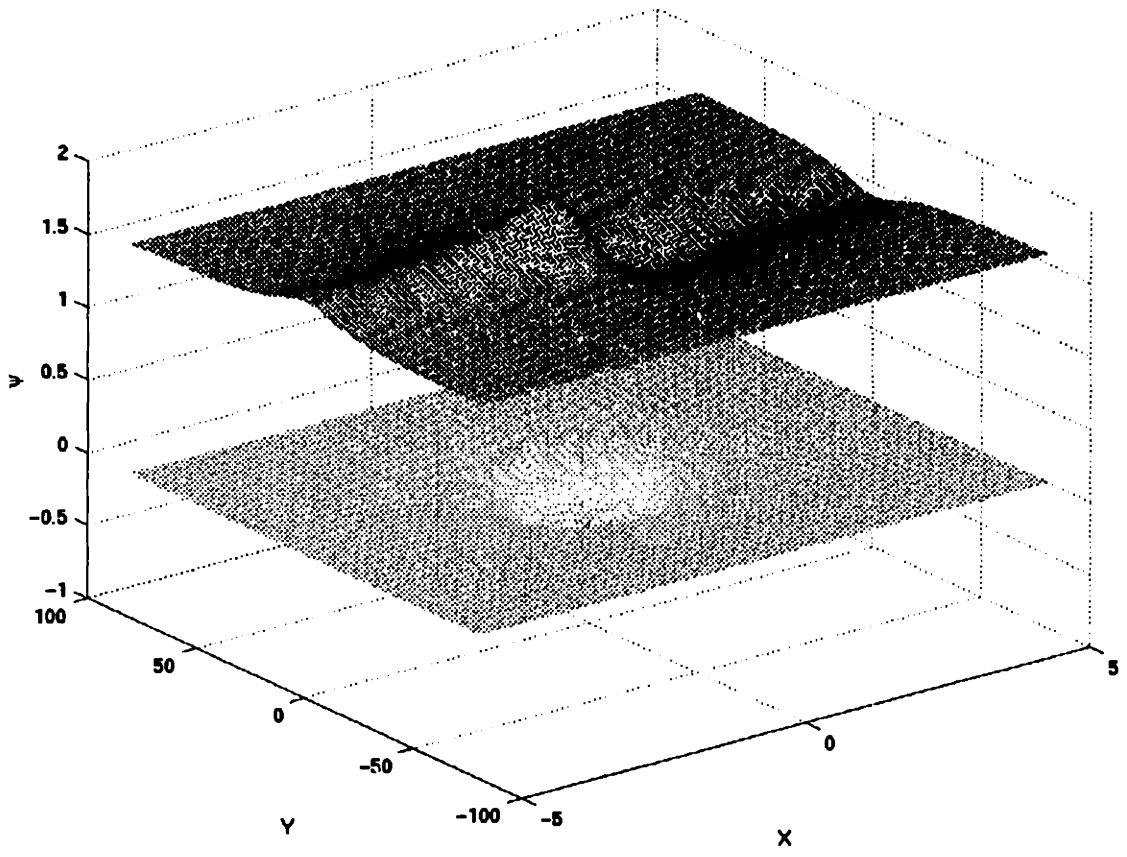


Figure 3.6: Streamfunction for actual three-dimensional solution with $L_x / L_y = 1/16$.

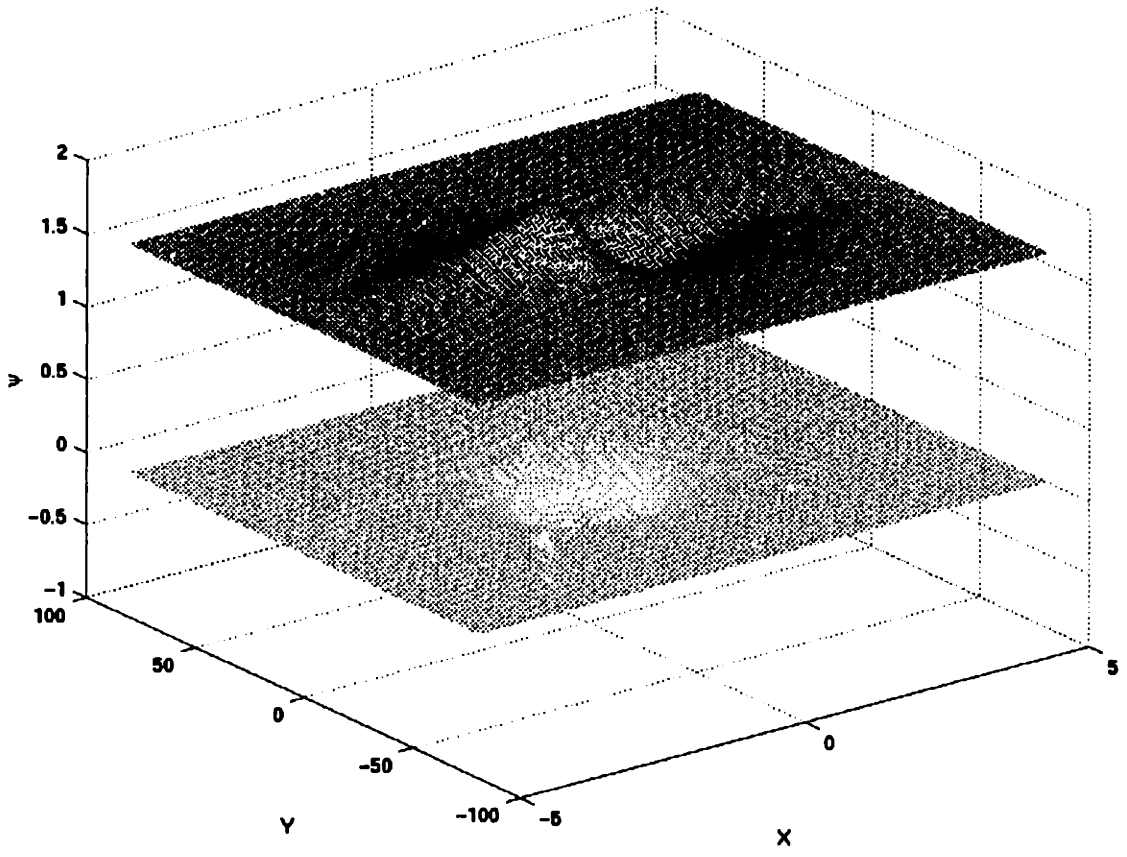


Figure 3.7: Streamfunction for two-dimensional approximation with $L_x / L_y = 1/16$.

# Chapter 4

# Closing Remarks

This chapter concludes the thesis by summarizing the findings and the methods developed from Chapter 2 and Chapter 3. In addition, this chapter also suggests possible avenues of future work in this area.

In this thesis, Long's model was extended to incorporate general stratification profiles for small and finite-amplitude two-dimensional flows as well as small-amplitude three-dimensional flows. This extension was accomplished by allowing for a solution that is only partially analytical. The general variation in the stratification is thereby resolved using a 'shooting' or integration technique. This additional numerical work is computationally inexpensive, yet results in a model that can incorporate realistic stratification profiles. For the finite-amplitude two-dimensional case, this method also converges for many situations that the two-layer method fails to converge. In addition, the general stratification allows for the study of the effect of the interfacial shape on tropopause tuning. As shown in this thesis, the tuning effects can be significantly diminished for an interface that continuously varies over a transition region in both the small and finite-amplitude cases.

There are many avenues for future work in related areas of stratified flow theory. The most profound area open for development is a concise analytical theory for finite-amplitude three-dimensional topography. Included in this area would be a study of the effect of three-dimensionality on finite-amplitude tropopause tuning. Subsequently, this area could be extended to general stratification as accomplished in this thesis for the finite-amplitude two-dimensional flow. Another avenue for future work is to use the general stratification method developed in

this thesis to study three or more layers of stratification. The occurrence of multiple layers leads to many interesting questions in regards to tropopause tuning. Perhaps the multiple tuning heights can cause constructive or destructive interference among the layers. Further avenues of future work also include relaxing the governing assumptions, such as the Bousinesq or hydrostatic approximations.

# Appendix A

# The Circulation Theorem

For the three-dimensional flow as described in Chapter 3, the circulation, $\Gamma$, can be introduced as

$$\Gamma = \int_{\tau} \mathbf{u} \cdot d\mathbf{r} = \iint_{S} \boldsymbol{\varpi} \cdot d\mathbf{S} . \tag{A.1}$$

Here, $\tau$ is a closed path of integration enclosing the area $S$. For a particular fluid particle, $\sigma$, $\mathbf{r}$ is the position vector, $\mathbf{u}$ is the velocity vector, and $\boldsymbol{\varpi}$ is the vorticity as defined in Equation 3.7. Expanding Equation A.1 gives

$$\Gamma = \int_{\tau} \mathbf{u} \cdot \frac{\partial \mathbf{r}}{\partial \sigma} d\sigma . \tag{A.2}$$

Taking the material derivative gives

$$\frac{D\Gamma}{Dt} = \int_{\tau} \left( \frac{D\mathbf{u}}{Dt} \cdot \frac{\partial \mathbf{r}}{\partial \sigma} + \mathbf{u} \cdot \frac{\partial^2 \mathbf{r}}{\partial \sigma \partial t} \right) d\sigma . \tag{A.3}$$

From the governing equations, the material derivative of the velocity is

$$\frac{D\mathbf{u}}{Dt} = -\frac{1}{\rho} \nabla p - \nabla(gz). \tag{A.4}$$

The symbol $p$ is the local pressure, $\rho$ is the local density, and $g$ is the gravitational acceleration. By definition, the local velocity vector is

$$\mathbf{u} = \frac{\partial \mathbf{r}}{\partial t} . \tag{A.5}$$

Substituting Equation A.4 and Equation A.5 in Equation A.3 gives

$$\frac{D\Gamma}{Dt} = -\int_{\tau}\left(\frac{1}{\rho}\nabla p + \nabla(gz)\right)\cdot dr + \frac{1}{2}\int_{\tau}\frac{\partial}{\partial\sigma}|\mathbf{u}|^2 d\sigma$$

$$= -\int_{\tau}\frac{1}{\rho}\nabla p \cdot d\mathbf{r} = \iint_{S}\frac{1}{\rho^2}(\nabla\rho\times\nabla p)\cdot d\mathbf{S}. \tag{A.6}$$

The governing equations state that the density following a fluid particle is constant. Therefore if $\tau$ is on a surface of constant density at $t=0$, then $\tau$ will always stay on this surface. Symbolically, this statement can be expressed as

$$\nabla\rho \| d\mathbf{S}. \tag{A.7}$$

Therefore, Equation A.6 becomes simply

$$\frac{D\Gamma}{Dt} = 0. \tag{A.8}$$

Assuming the flow starts from rest, the circulation becomes

$$\Gamma = 0. \tag{A.9}$$

Substituting this result in Equation A.1 gives

$$\iint_{S}\varpi\cdot d\mathbf{S} = 0. \tag{A.10}$$

This expression in turn gives the result

$$\varpi\cdot\nabla\rho = 0. \tag{A.11}$$

# References


BAINES, P. G. 1977. Upstream influence and Long's model in stratified flows. *J. Fluid Mech.* **82**, 147.

BAINES, P. G. 1987. Upstream blocking and airflow over mountains. *Ann. Rev. Fluid Mech.* **19**, 75.

BAINES, P. G. 1995. *Topographic effects in stratified flows.* Cambridge University Press, New York.

DRAZIN, P. G. 1961. On the steady flow of a fluid of variable density past an obstacle. *Tellus.* **13**, 239.

DRAZIN, P. G. & MOORE, D. W. 1967. Steady two-dimensional flow of fluid of variable density over an obstacle. *J. Fluid Mech.* **28**, 353.

DRAZIN, P. G. & REID, W. H. 1981. *Hydrodynamic Stability.* Cambridge University Press.

DURRAN, D. R. 1992. Two-Layer solutions to Long's equation for vertically propagating mountain waves: how good is linear theory? *Q. J. R. Meteorol. Soc.* **118**, 415.

KLEMP, J. B. & LILLY, D. K. 1975. The dynamics of wave-induced downslope winds. *J. Atmos. Sci.* **32**, 320.

LILLY, D. K. & KLEMP, J. B. 1979. The effects of terrain shape on nonlinear hydrostatic mountain waves. *J. Fluid Mech.* **95**, 241.

LONG, R. R. 1953. Some aspects of the flow of stratified fluids. I. A theoretical investigation. *Tellus.* **5**, 42.

LONG, R. R. 1955. Some aspects of the flow of stratified fluids. III. Continuous density gradients. *Tellus.* **7**, 341.

LONG, R. R. 1959. The motion of fluids with density stratification. *J. Geophys. Res.* **64**, 2151.

MCINTYRE, M. E. 1972. On Long's hypothesis of no upstream influence in uniformly stratified or rotating flow. *J. Fluid Mech.* **52**, 209.

MILES, J. W. 1969. Waves and wave drag in stratified flows. *Proc. 12$^{th}$ Intl. Congress of Applied Mechanics*, Springer, Berlin.

PELTIER, W. R. & CLARK, T. L. 1983. Nonlinear mountain waves in two and three spatial dimensions. *Q. J. R. Meteorol. Soc.* **109**, 527.

SMITH, R. B. 1980. Linear theory of stratified hydrostatic flow past an isolated mountain. *Tellus*. **32**, 348.

SMITH, R. B. 1989. Hydrostatic airflow over mountains. *Advances in Geophysics*. **31**, 1.

YIH, C.-S. 1960. Exact Solutions for steady two-dimensional flow of a stratified fluid. *J. Fluid Mech.* **9**, 161.

YIH, C.-S. 1967. Equations governing steady two-dimensional large-amplitude motion of a stratified fluid. *J. Fluid Mech.* **29**, 539.

YIH, C.-S. 1980. *Stratified Flows*. Academic Press, Inc., New York.